Molecular Biology of the Cell
Vol. 9, 1495–1512, June 1998

The Endogenous and Cell Cycle-dependent Phosphorylation of tau Protein in Living Cells: Implications for Alzheimer's Disease

Susanne Illenberger, Qingyi Zheng-Fischhöfer, Ute Preuss,* Karsten Stamer, Karlheinz Baumann,† Bernhard Trinczek, Jacek Biernat, Robert Godemann, Eva-Maria Mandelkow, and Eckhard Mandelkow‡

Max-Planck-Unit for Structural Molecular Biology, D-22603 Hamburg, Germany

Submitted October 14, 1997; Accepted March 23, 1997
Monitoring Editor: J. Richard McIntosh

In Alzheimer's disease the neuronal microtubule-associated protein tau becomes highly phosphorylated, loses its binding properties, and aggregates into paired helical filaments. There is increasing evidence that the events leading to this hyperphosphorylation are related to mitotic mechanisms. Hence, we have analyzed the physiological phosphorylation of endogenous tau protein in metabolically labeled human neuroblastoma cells and in Chinese hamster ovary cells stably transfected with tau. In nonsynchronized cultures the phosphorylation pattern was remarkably similar in both cell lines, suggesting a similar balance of kinases and phosphatases with respect to tau. Using phosphopeptide mapping and sequencing we identified 17 phosphorylation sites comprising 80–90% of the total phosphate incorporated. Most of these are in SP or TP motifs, except S214 and S262. Since phosphorylation of microtubule-associated proteins increases during mitosis, concomitant with increased microtubule dynamics, we analyzed cells mitotically arrested with nocodazole. This revealed that S214 is a prominent phosphorylation site in metaphase, but not in interphase. Phosphorylation of this residue strongly decreases the tau–microtubule interaction in vitro, suppresses microtubule assembly, and may be a key factor in the observed detachment of tau from microtubules during mitosis. Since S214 is also phosphorylated in Alzheimer's disease tau, our results support the view that reactivation of the cell cycle machinery is involved in tau hyperphosphorylation.

INTRODUCTION

Microtubule-associated proteins (MAPs)[1] are key factors regulating microtubule dynamics in living cells. These proteins bind to microtubules in a nucleotide-insensitive way, leading to an overall stabilization of the microtubule network. Microtubules are involved in highly dynamic cellular events: they drive neurite outgrowth and are responsible for correct chromosome segregation at mitosis (reviewed by Kosik and McConlogue, 1994; Schoenfeld and Obar, 1994; Hyman and Karsenti, 1996). There is much evidence that the modulation of the MAP–microtubule interaction is regulated by the phosphorylation state of MAPs. Tau protein, a class of mammalian MAPs in brain, is predominantly found in the axons of neurons (Binder *et al.*, 1985), where it is thought to support axonal transport by stabilizing axonal microtubules. As in the related proteins MAP2 and MAP4, the microtubule-binding region of tau (Figure 1) is located in the C-terminal half of the protein. It includes three or four

* Present address: Institute of Genetics, University of Bonn, D-53117 Bonn, Germany.
† Present address: Nervous System Research, Novartis Pharma Inc., CH-4002 Basel, Switzerland.
‡ Corresponding author. E-mail address: mandelkow.mpasmb.desy.de.
[1] Abbreviations: AD, Alzheimer's disease; GFP, green fluorescent protein; GSK-3, glycogen synthase kinase-3; MAPs, microtubule-associated proteins; PHFs, paired helical filaments; TLE/TLC, thin layer electrophoresis/TLC.

pseudorepeats of ~31 residues each depending on the isoform (Lee *et al*., 1988; Goedert *et al*., 1989; Himmler *et al*., 1989). The repeats are flanked by basic, proline-rich stretches that help to target the protein to the microtubule (Butner and Kirschner, 1991; Brandt *et al*., 1994; Goode and Feinstein, 1994; Gustke *et al*., 1994). The N-terminal part of the molecule is more acidic and does not interact with microtubules (projection domain). In Alzheimer's disease (AD), tau becomes detached from microtubules and aggregates into the paired helical filaments (PHFs), a hallmark in the AD neurofibrillary pathology (review by Kosik and Greenberg, 1994). Tau isolated from these aggregates is highly phosphorylated, about 4 times as much as tau from brain tissue of nondemented individuals (Ksiezak-Reding *et al*., 1992; Köpke *et al*., 1993). Mapping of phosphorylation sites of PHF-tau by mass spectrometry revealed that many of the residues phosphorylated are of the Ser-Pro/Thr-Pro type, predominantly located in the proline-rich region (Morishima-Kawashima *et al*., 1995). Some of these can be detected with phosphorylation-dependent antibodies (reviewed by Kosik and Greenberg, 1994; Mandelkow *et al*., 1995).

There is increasing evidence that mitotic mechanisms may be involved in the abnormal phosphorylation of tau in AD neurons: 1) Tau from fetal brain tissue, still undergoing cell division, has an elevated phosphate content and is recognized by diagnostic phosphorylation-dependent AD antibodies (Kanemaru *et al*., 1992; Brion *et al*., 1993; Kenessey and Yen, 1993, Matsuo *et al*., 1994). 2) In several cell lines the phosphorylation of tau is increased specifically during mitosis (Pope *et al*., 1994; Preuss *et al*., 1995; Vincent *et al*., 1996; Preuss and Mandelkow, 1998). 3) There is a tight link between apoptosis and the cell cycle machinery (for reviews see Pandey and Wang, 1995; King and Cidlowski, 1995) and induction of mitosis in postmitotic neuronal cells leads inevitably to cell death (Park *et al*., 1996). 4) Furthermore, apoptosis is indeed elevated in hippocampal brain tissue in AD (Smale *et al*., 1995; Li *et al*., 1997). A current hypothesis for the AD-specific phosphorylation of tau therefore states that the affected neurons try to reenter the proliferative phase as a result of some hitherto unknown insult. Thus, turning on the "inappropriate" program ultimately drives the cells into apoptosis, explaining the massive loss of neurons from AD brains.

Many of the investigations of tau phosphorylation in living cells have concentrated on immunocytochemical detection of phosphorylation sites with diagnostic AD antibodies, thus limiting the analysis to those sites where antibodies were available (reviewed by Friedhoff and Mandelkow, 1998). To overcome these limitations we have analyzed tau from metabolically radiolabeled cells by two-dimensional (2D) phosphopeptide mapping. This approach allows the detection of all phosphorylation sites, including those not seen by antibody labeling, and allows relative quantification (Boyle *et al*., 1991). We investigated two cell lines in parallel, the LAN-5 neuroblastoma cells (Seeger *et al*., 1982) that express moderate levels of tau protein endogenously (Greenwood and Johnson, 1995), and a Chinese hamster ovary (CHO) cell line stably transfected with the longest human tau isoform (htau40; Preuss *et al*., 1995). Using recombinant tau protein phosphorylated in vitro with different kinases to generate reference phosphopeptides, we identified the 17 major in vivo phosphorylation sites in the two cell lines corresponding to 80–90% of the total radiolabel incorporated. The overall pattern in the neuronal and nonneuronal cells was remarkably similar, showing that transfected CHO cells can function as a cell model to study tau phosphorylation. Most of the sites are of the Ser-Pro/Thr-Pro type except S214 and S262. Transfected CHO cells arrested in metaphase show enhanced phosphorylation in several peptides, including T153, T181, S202/T205, T212/T217, and S214. The first four peptides are phosphorylated by cdc2 in vitro, suggesting that this kinase could be involved in the phosphorylation of MAPs during mitosis. S214 can be rapidly and selectively phosphorylated in vitro by PKA, and this single site strongly affects tau's ability to bind and stabilize microtubules. Thus, phosphorylation at S214 by PKA or an equivalent kinase could contribute to the increase in microtubule dynamics during mitosis. In addition, S214 has recently been shown to be part of the epitope of the antibody AT 100 that specifically recognizes PHF-tau (Hoffmann *et al*., 1997; Zheng-Fischhöfer *et al*., 1998). The knowledge of the physiological phosphorylation sites will be also applicable to primary neurons to monitor the changes in tau phosphorylation due to various insults (e.g., amyloid toxicity, oxidative stress).

MATERIALS AND METHODS

Proteins

Human tau cDNA clones were kindly provided by M. Goedert (Goedert *et al*., 1989), mitogen-activated protein kinase (MAPK) and its activating kinase (MEK) were kindly provided by F. Döring and B. Berling (Döring *et al*., 1993). Proteins were expressed in *Escherichia coli* using variants of the pET vector (Studier *et al*., 1990). Recombinant tau protein was purified by making use of its heat stability and by Mono S fast protein liquid chromatography (Hagestedt *et al*., 1989). MAP/microtubule affinity-regulating kinase (MARK) and the neuronal cdc2-like kinase cdk5 were prepared from porcine brain as described previously (MARK, Drewes *et al*., 1995; cdk5, Baumann *et al*., 1993). GSK-3β was expressed in active form in *E. coli* following the procedure of Wang *et al*. (1994); the original clone was generously provided by J.R. Woodgett. cAMP-dependent protein kinase (PKA) was obtained from Promega (Madison, WI).

The kinase cdc2 was immunoprecipitated from HeLa-S3 cells after mitotic arrest with 0.4 μg/ml nocodazole. Cells were initially lysed in hypotonic 10 mM phosphate buffer (pH 7.0) containing 5 mM $MgCl_2$, 1 mM EDTA, 1 mM EGTA, 10 mM NaF, 10 mM β-glycerophosphate, 1 mM PMSF, 1 μg/ml leupeptin, 1 μg/ml

pepstatin, 1 μg/ml aprotinin. After the addition of 0.5 M NaCl (final concentration) and further homogenization, the homogenate was centrifuged at 4°C for (148,000 × *g*). The supernatant was dialyzed against SP-Sepharose buffer A (50 mM 2-(*N*-morpholino)ethanesulfonic acid, pH 6.5, 2 mM EGTA, 0.5 mM dithiothreitol, 0.2 mM PMSF, 3 mM $MgCl_2$, 0.5 mM benzamidine, 0.2 mM sodium vanadate, 0.02 mM sodium fluoride, 0.01% Brij 35), loaded onto a SP-Sepharose column, and eluted in 40 ml buffer B (buffer A with 0.5 M NaCl). Fractions (2 ml) were assayed for cdc2 activity on phosphocellulose paper discs (Life Technologies, Gaithersburg, MD) (Casnellie, 1991), using the modified histone H1 peptide PKTPKKAKKL as substrate (Beaudette *et al*., 1993). Active fractions were pooled and immunoprecipitated with an anti-cyclinB-antibody (generous gift from G. Draetta, Mitotix, Cambridge, MA).

Construction of the GFP-tau Vector

The multicloning site in the pEGFP-N1 vector (Clontech, Palo Alto, CA) upstream of GFP was removed with the restriction endonucleases *Nhe*I and *Bam*HI. Oligonucleotides carrying *Xba*I and *Bgl*II restriction sites were ligated into the open frame to omit the *Nhe*I and *Bam*HI restriction sites. To create a new multicloning site downstream of GFP, the vector was cut open with Bsp1407 I and *Not*I. 36-oligomers containing *Nde*I, *Esp*I, *Nhe*I, and *Bam*HI restriction sites were inserted. Tau protein was excised from a bacterial expression vector (pNG2; Gustke *et al*., 1994) and cloned into the *Nde*I *Bam*HI site to gain a fusion protein with GFP fused to the N terminus of tau.

Transfection

CHO cells were plated onto LabTek chambered cover glass (NUNC, Naperville IL) at 70% confluency the day before transfection. Transfection was carried out with Dotap (Boehringer, Mannheim, Germany) according to manufacturer's instructions.

Phosphorylation Reactions

Phosphorylation reactions were carried out in 40 mM HEPES (pH 7.2) containing 10 μM tau protein, 5 mM $MgCl_2$, 2 mM dithiothreitol, 5 mM EGTA, 0.2 mM PMSF, and 1 mM [γ^{32}P]-ATP (100–200 Ci/mol). Phosphorylation was assayed in SDS gels (Steiner *et al*., 1990).

Cell Culture

CHO cells stably transfected with the longest human tau isoform htau40 (Preuss *et al*., 1995) or with a GFP-htau40 construct were grown in HAM's F12 medium supplemented with 10% FCS (Biochrom, Berlin, Germany) in the presence of 600 μg/ml Geneticin (G-418). LAN-5 human neuroblastoma cells (Seeger *et al*., 1982) and HeLa-S3 cells were grown in RPMI 1640 medium supplemented with 10% FCS. HeLa-S3 cells grown in spinner cultures were mitotically arrested by overnight treatment with 0.4 μg/ml nocodazole (Sigma, Deisenhofen, Germany).

Cell Extracts

For Western blot analysis of tau protein only, total cell extracts of CHO cells transfected with htau40 and LAN-5 neuroblastoma cells were prepared by lysing subconfluent cells on ice in a hypotonic buffer containing 50 mM Tris (pH 7.4), 2 mM EGTA, 2 mM EDTA, 20 mM NaF, 0.1 mM PMSF, 1 μg/ml leupeptin, 1 μg/ml aprotinin, 1 μg/ml pepstatin, 10 mM benzamidine, 1 μM microcystine, and 0.1 M ocadaic acid. Extracts were centrifuged immediately at 15,800 × *g* for 10 min at 4°C. Supernatants were treated with perchloric acid (2.5% final concentration) for 15 min at room temperature. After centrifugation (15,800 × *g* for 10 min at 4°C) tau protein remaining in the supernatant was precipitated with trichloroacetic acid (15% final concentration, 15 min on ice) and centrifuged (15,800 × *g* for 10 min at 4°C). Trichloroacetic acid pellets were either resuspended directly in sample buffer or, for dephosphorylation with alkaline phosphatase, they were washed with ice-cold ethanol, air-dried, and dephosphorylated according to manufacturer's instructions. Samples were run on 10% SDS gels. To analyze the tau and tubulin content of interphase and nocodazole-treated cells without and after extraction, cells were treated with 1% Triton-X 100 in an MT-stabilizing buffer (MTSB: 80 mM piperazine-*N*,*N*′-bis(2-ethanesulfonic acid), pH 6.9, 1 mM $MgCl_2$, 1 mM EGTA, 4% polyethyleneglycol) for 10 s. Triton and the extracted proteins were removed by a brief wash in MTSB and subsequent lysis in hypotonic buffer. After centrifugation (15,800 × *g* for 10 min at 4°C) SDS sample buffer was added to the supernatants.

SDS-PAGE and Western Blotting

Extract samples were electrophoresed on 10% SDS-polyacrylamide gels (perchloric acid-soluble fraction from 1×10^6 CHO cells and 1×10^7 LAN-5 cells, respectively, per lane) and transferred electrophoretically to polyvinylidene difluoride membranes (Millipore, Eschborn, Germany). Residual membrane-binding sites were blocked with 5% nonfat dry milk in Tris-buffered saline after incubation with the monoclonal antibody T46 (1:6000). Bound antibody was detected with a peroxidase-conjugated antibody and visualized using ECL according to manufacturer's instructions (Amersham-Buchler, Braunschweig, Germany). Densitometric analysis was carried out using the TINA 2.09f software from Raytest GmbH (Straubenhardt, Germany). For immunoblot analysis, recombinant htau23 and htau40 from *E. coli* were isolated by fast protein liquid Mono S (Pharmacia, Freiburg, Germany) chromatography on the basis of its heat stability (for details see Hagestedt *et al*., 1989).

Immunofluorescence and Microscopy

Cells were washed in an MTSB (80 mM piperazine-*N*,*N*′-bis(2-ethanesulfonic acid), pH 6.9, 1 mM $MgCl_2$, 1 mM EGTA, 4% polyethyleneglycol) and subsequently fixed in methanol (5 min at −20°C). For extraction experiments, cells were extracted with 1% Triton-X 100 in MTSB for 10 s before methanol fixation. Time and fixative were crucial for differential extraction. Prolonged incubation with Triton-X 100 almost completely removed tau protein from all cells irrespective of cell cycle stage and also affected cellular microtubules (our unpublished observations). Paraformaldehyde fixation was not applicable, since the cellular localization of tau is altered: instead of colocalizing with microtubules, tau protein is distributed throughout the cytoplasm, a phenomenon that has been described previously (Schliwa *et al*., 1981). Hence, only methanol fixation represented the in vivo distribution of tau as was determined by live observation of EGFP-Tau-expressing CHO cells. The rabbit polyclonal anti-tau antibody (Dako, Hamburg, Germany) and the monoclonal anti-α-tubulin antibody DM1A (Sigma, Deisenhofen, Germany) were used at 1:300 and 1:200 dilutions, respectively. Fluorescently labeled (FITC and TRITC) secondary antibodies were obtained from Dianova (Hamburg, Germany). Samples were examined using an Axioplan fluorescence microscope (Zeiss, Jena, Germany). Pictures were taken with a cooled CCD camera (Visicam, Visitron, Puchheim, Germany) using the MetaMorph software package (Visitron). In vivo observation of cells transfected with GFP-htau40 was conducted with an inverted Axiovert 10 microscope (Zeiss) using filters for FITC fluorescence.

Metabolic Labeling and Immunoprecipitation

Both stably transfected CHO cells and LAN-5 neuroblastoma cells grown in 75-cm^2 culture flasks were preincubated for 60 min in phosphate-free MEM (Life Technologies) containing 10% FCS dialyzed against 20 mM HEPES. Subsequently [^{32}P]-orthophosphate (0.7 mCi/ml) was added to the media and cells were then incubated for 4 h. Cells were lysed on ice in the hypotonic 10 mM phosphate buffer (pH 7.0) described above and immediately centrifuged at 15,800 × *g* for 10 min. The supernatant was boiled for 5 min and again centrifuged at 15,800 × *g* for 10 min. (15 μg) Polyclonal rabbit

anti-Tau antibody (Dako) was added and incubated under constant agitation at 4°C for 2 h. (50 μl) Protein-A/G-Sepharose beads (Dianova, Hamburg, Germany) were added and incubation was continued overnight. The immune complexes were recovered by centrifugation and rinsed four times in immunoprecipitation buffer. To arrest CHO cells in metaphase, 0.4 μg/ml nocodazole (Sigma) was added to the phosphate-free medium (DeBrabander *et al*., 1986). Mitotic cells were detached by mechanical shake-off. Lysis of cells and immunoprecipitation were carried out as described above.

Sequencing and Mass Spectrometric Analysis of Peptides

Fractionated peptides were sequenced on a 476-A Liquid Phase Protein Sequencer (Applied Biosystems, Weiterstadt, Germany). Mass spectrometry was performed using a MALDI II instrument (Matrix Assisted Laser Desorption/Ionization, Shimadzu, Duisburg, Germany). Phosphorylated serine was determined by the formation of the dithiothreitol adduct of dehydroalanine (Meyer *et al*., 1993). Phosphothreonine was determined by the loss of the threonine peak in the sequence and by the 80-Da mass increase (as seen by MALDI) due to the incorporated phosphate.

Phosphopeptide Mapping by Thin-Layer Electrophoresis/Chromatography and HPLC

After in vitro phosphorylation, kinase proteins were removed by boiling the samples in 0.5 M NaCl, 5 mM dithiothreitol and centrifugation. Tau remains in the supernatant and was precipitated by 15% trichloroacetic acid on ice. Tau protein immunoprecipitated from cells was resolubilized in SDS-sample buffer and boiled for 5 min. Electrophoresis was carried out on a 10% SDS polyacrylamide gel, and the unstained gel was subjected to autoradiography to identify labeled tau protein. Tau bands were cut out of the gel and eluted overnight in 50 mM NH_4HCO_3 buffer (pH 7.4) containing 0.1% SDS and 5% β-mercaptoethanol. Before precipitation by 15% trichloroacetic acid, 20 μg recombinant htau 40 were added. Cysteine residues were modified by performic acid (Hirs, 1967). The protein was digested overnight with trypsin (Promega, sequencing grade) in the presence of 0.1 mM $CaCl_2$, using two additions of the enzyme in a ratio of 1:10–1:20 (wt/wt).

2D phosphopeptide mapping on thin-layer cellulose plates (Macherey and Nagel, Düren, Germany) was performed according to Boyle *et al*. (1991). First-dimension electrophoresis was carried out at pH 1.9 in formic acid (88%)/glacial acetic acid/water (50:156:1794), second-dimension chromatography at pH 3.5 in n-butyl alcohol/pyridine/glacial acetic acid/water (150:100:30:120). For the mapping of phosphorylation sites by sequencing, 400 μg of recombinant htau40 were phosphorylated with cdc2, cdk5, MEK/MAPK, and GSK-3β in the presence of 1 mM [γ^{32}P]-ATP (150 Ci/mol) for 16 h. Samples were treated as described above and digested with trypsin. Separation of peptides was performed by HPLC on a Vydac 218TP52 column using a gradient of 0% acetonitrile, 0.075% trifluoroacetic acid to 50% acetonitrile, 0.05% trifluoroacetic acid in 150 min with a flow rate of 80 μl/min (Smart System, Pharmacia). Radioactive fractions were rechromatographed on a μRPC C2/C18 SC2.1/10 column (Pharmacia) using a gradient of 0% acetonitrile, 0.075% trifluoroacetic acid to 50% acetonitrile, 0.05% trifluoroacetic acid in 60 min with a flow rate of 0.1 ml/min. Sequence analysis of peptides was performed using 476-A pulsed liquid phase sequencer and a 120-A online phenylthiohydantoin-derivative analyzer (Applied Biosystems). Phosphoserines and -threonines were modified with ethanethiol before sequencing and subsequently identified as *S*-ethylcysteine and β-methyl-*S*-ethylcysteine, respectively (Meyer *et al*., 1993). For the case of phosphorylation by GSK-3β, 100 μg of htau40 were phosphorylated with [γ^{32}P]-ATP, digested with trypsin, and separated on 10 TLC plates (10 μg peptide mix per plate). The peptide spots were then scratched out of the plates and recovered as described by Boyle *et al*. (1991) and further purified on a Vydac reverse phase column. The radioactive fractions were then analyzed by MALDI and sequencing.

Phosphoamino Acid Analysis

Aliquots of digestion samples were partially hydrolyzed in 6 N HCl (110°C, 60 min) and analyzed by 2D electrophoresis at pH 1.9 and pH 3.5 according to Boyle *et al*. (1991).

Tau-Microtubule Binding Assay

Binding curves between tau and microtubules were obtained as described (Gustke *et al*., 1994). Microtubules were stabilized by taxol, which allows one to measure binding independently of microtubule dynamics. Microtubule-bound and free tau fractions were separated by centrifugation, run on SDS gels, and stained with Coomassie brilliant blue R250. The gels were scanned on an HP ScanJet 4c and evaluated with the Tina 2.0 software (Raytest, Straubenhardt, Germany). The data can be fitted by nonlinear regression using the standard binding equation for a macromolecule containing equivalent and noninteracting ligand-binding sites: $[Tau_{bound}] = n[Mt_o][Tau_{free}]/\{K_d + [Tau_{free}]\}$.

Video Microscopy of Microtubule Assembly

This was done as described previously (Trinczek *et al*., 1995): 25 μM PC-tubulin and 10 μM tau isoforms or constructs were mixed. A portion of the samples (0.5 μl) was put on a slide, covered with 18 × 18 mm coverslips, sealed, and warmed up to 37°C with a controlled air flow within 5 s. Observation began ~15 s after temperature shift to 37°C; the number of microtubules per volume of the monitor field was recorded by focussing through the whole depth of the field and counted later from the video frames. Each assay was done for 10 fields and repeated three times. The monitor field contained an area of 73 × 54 μm^2 (~4000 μm^2), the depth of the solution was ~3–4 μm, and focal depth was ~1–2 μm.

RESULTS

Expression and Phosphorylation of tau in Nonsynchronized LAN-5 and CHO Cells

The major function of the neuronal MAP tau is to bind to and hence stabilize axonal microtubules. This is important for maintaining axonal transport and defining the polarity of a neuron. Tau protein can roughly be subdivided into two domains, the N-terminal projection domain, followed by the C-terminal microtubule-binding domain (Figure 1). Phosphorylation is thought to be the key factor regulating tau–microtubule interaction. Earlier studies on tau phosphorylation have shown that tau protein can be phosphorylated by several kinases in vitro and that most phosphorylation sites lie in the microtubule-binding domain. Several of these sites are recognized by phosphorylation-dependent antibodies that have been used to characterize Alzheimer tau and to monitor phosphorylation in living cells (reviews by Johnson and Jenkins, 1996; Friedhoff and Mandelkow, 1998). However, the immunocytochemical detection of phosphorylation sites is limited to the antibodies available. We therefore used 2D phosphopeptide mapping of metabolically radiolabeled cells to visualize all phosphopeptides present. In addition, the amount of radio-

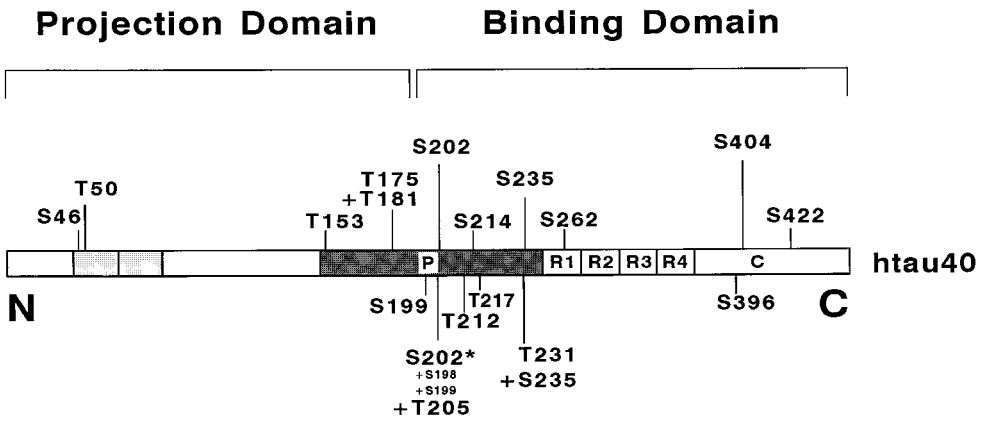

Figure 1. Bar diagram of the longest human tau isoform (htau40) in human CNS, used for transfection of CHO cells in this study. The identified phosphorylation sites are shown. Tau protein can be subdivided into an N-terminal projection domain and a C-terminal binding domain. Only the latter interacts with microtubules. It contains three or four repeats (R1-R4) that are flanked N-terminally by a proline-rich region (P) that extends into the projection domain and harbors most of the Ser/Thr-Pro motifs. The six tau isoforms in human CNS are generated by alternative splicing (0, 1, or 2 inserts near the N terminus shown as shaded boxes, and repeat R2 present or absent). The endogenous tau in LAN-5 cells consists of only two isoforms, htau23 and htau24 (no inserts, repeat R2 absent or present). The identified phosphorylation sites are located mainly in the proline-rich region upstream of the repeats. Except for S214, all of these sites are of the proline-directed type. The only KXGS motif found to be phosphorylated in vivo is S262 located in the first repeat.

label incorporated can be used for relative quantification.

LAN-5 cells (a human neuroblastoma cell line; Seeger *et al.*, 1982) express the two smallest tau isoforms, htau23 and htau24, endogenously (Figure 2, lanes 4,5). This is sufficient for analysis if a large number of cells are averaged without regard to stages of the cell cycle. However, to monitor tau phosphorylation in different stages of the cell cycle, we had to turn to CHO cells stably transfected with tau (htau40 isoform, Figure 2, lane 2) which express 5–10 times the amount of tau compared with LAN-5 cells (200–300 ng tau/10^7 cells in CHO cells, compared with 20–50 ng/10^7 LAN-5 cells). The justification for using transfected CHO cells overexpressing tau protein as a model for cells of neuronal origin comes from the similarity of their tau phosphorylation patterns (as shown below). Judging from Western blots, the phosphorylation of tau in both cell lines generates several subspecies of each isoform that migrate at higher apparent Mr values (Figure 2, lanes 2 and 4), but dephosphorylation with alkaline phosphatase increases the electrophoretic mobility to that of the corresponding recombinant proteins expressed in *E. coli* (shown for LAN-5 in Figure 2, lane 5). The Mr shift is a rough indicator of phosphorylation but cannot be used to quantify the extent since the various phosphorylation sites differ greatly in their effect on the electrophoretic mobility of tau in the gel (Lichtenberg-Kraag *et al.*, 1992).

When LAN-5 cells were metabolically labeled with [^{32}P]-orthophosphate (0.7 mCi/ml) for 4 h, their 2D maps of tau phosphopeptides revealed a complex pattern of 23 individual spots (Figure 3a). For CHO cells this procedure yielded a surprisingly similar map in spite of the different origins of these cell types and the different isoforms expressed (Figure 3b). Some minor spots occurring in CHO, but not in LAN-5, cells are due to the phosphorylation of S46 and T50 in the additional inserts present in htau40. The two maps are similar not only in terms of signals detected, but also in their relative intensities (Table 1). This is strong evidence that the balance of kinases and phosphatases is similar in the two cell lines. The major spots correspond to peptides S396/S404, T175/T181, S202, S202/T205* (peptide S195-R209 with two phosphate groups, one at S202, the other at either T205 or S199 or S198), S235, and S404. As additional phosphopeptides we found T153, T181, S199, T212, S214, T217, T231/S235, S262, and S422 (for identification see below and Figure 6). All identified signals together comprise 88% of the incorporated phosphate in CHO cells, and 78% in LAN-5 cells (Table 1 and Illenberger, unpublished results). The most intense signal in both peptide maps (Ser396/Ser404, Figure 3, a and b) contained 31% and 24%, respectively, leaving only a residual 12% (CHO) and 22% (LAN-5) phosphate incorporated into a few minor unidentified phosphopeptides. Note, however, that the total extent of phosphorylation cannot be obtained from the maps because nonphosphorylated peptides cannot be detected with this method. It is probably much smaller than suggested by the number of sites; from immunocytochemical analyses with phosphorylation-dependent antibodies we estimate that the average tau molecule contains about two to three phosphates in

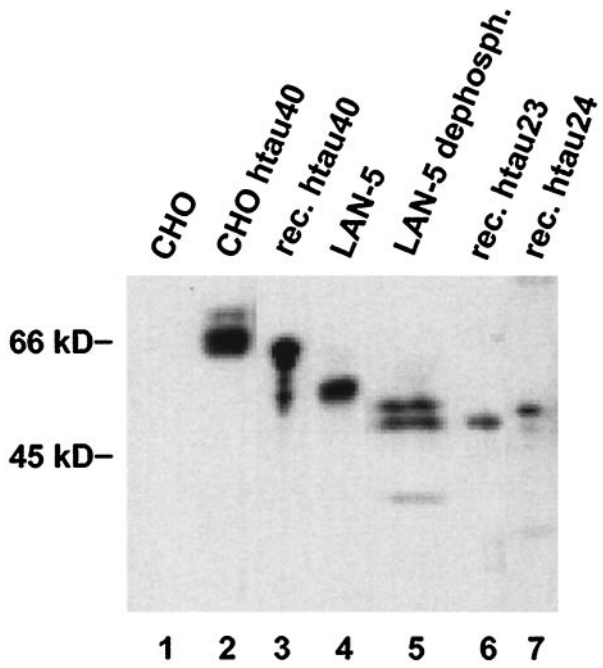

Figure 2. Western blot analysis of tau protein in stably transfected CHO cells and LAN-5 neuroblastoma cells. Lane 1, nontransfected CHO cells, showing that there is no endogenous tau; lane 2, CHO cells stably transfected with htau40. There are bands of higher Mr representing different phosphorylation states of the protein. Lane 3, recombinant htau40 (longest human tau isoform, 441 residues), showing a single band at Mr 65 kDa; lane 4, tau isolated from LAN-5 neuroblastoma cells. Lane 5, tau from LAN-5 cells after dephosphorylation with alkaline phosphatase, showing two bands that comigrate with htau23 (lower) and htau24 (upper) indicating that LAN-5 cells contain these two isoforms (3 or 4 repeats, no N-terminal inserts) and their phosphorylated derivatives. Lane 6, recombinant fetal tau (htau23, 352 residues); lane 7, recombinant htau24 (383 residues).

LAN-5 cells and probably even less in CHO cells (apart from mitosis, see below).

Tau Phosphorylation in Interphase and in Mitotically Arrested CHO Cells

In a previous immunocytochemical study we had shown that in stably transfected CHO cells tau protein becomes highly phosphorylated during mitosis (sevenfold increase), which appeared to correlate with the detachment of tau from the microtubules and the rearrangement of the microtubule network (Preuss *et al*., 1995). To further analyze the tau–microtubule interaction, we observed living CHO cells expressing a GFP-tau fusion protein. The microtubule network is stained in interphase cells due to GFP-tau binding to cellular microtubules (Figure 4a, left panel) in agreement with Ludin *et al*. (1996). In mitotic cells (Figure 4a, right panel) the green fluorescence is mainly distributed throughout the whole cytosol with some more intense staining of the mitotic spindle, suggesting that a significant amount of tau protein becomes detached from microtubules. To be able to visualize tau and microtubules at the same time, we performed indirect immunofluorescence in stably transfected CHO cells expressing the longest human tau isoform, htau40 (Preuss *et al*., 1995). Cells were fixed in methanol, either without prior extraction of cytosolic proteins or after treatment for 10 s with 1% Triton-X 100 (Figure 4b). In untreated interphase cells, tau protein colocalizes with microtubules. In mitotic cells, however, there is pronounced tau staining in the cytosol in addition to staining of the mitotic spindle (Figure 4b, upper right panel), similar to mitotic living cells expressing GFP-tau (compare Figure 4a, right panel). If cytosolic proteins were removed by brief extraction with Triton-X 100 (Figure 4b, lower two panels; according to the procedure of Melan and Sluder, 1992), the distribution of tau in interphase cells was not altered, whereas in mitotic cells the cytosolic tau staining had disappeared. Only tau bound to spindle microtubules remained in these cells (Figure 4b, lower right panel). This result further indicated that a significant fraction of tau protein did not bind to microtubules during mitosis. The fixation procedure was crucial for the demonstration of this effect. Prolonged extraction washed out all tau protein from the cell. Paraformaldehyde, for some reason, detaches tau from microtubules (also described by Schliwa *et al*., 1981) abolishing the colocalization of tau and microtubules.

To get a more quantitative estimate of the changes in the binding of tau during mitosis, we performed a Western blot analysis of cell extracts from nonsynchronized (interphase) and nocodazole-treated (M-phase) cells and compared the tau and tubulin levels before and after Triton extraction (Figure 4c). Western blots were analyzed densitometrically to asses relative tau to tubulin ratios. The amount of tubulin between untreated and extracted cell pellets did not significantly change throughout the cell cycle (lanes 1–4), indicating that the nonextractable polymer mass of tubulin essentially remains the same. In interphase cells, Triton extraction had no effect on the amount of tau remaining in the pellet, indicating that most tau protein in interphase cells is bound to microtubules (lanes 6 and 7). In contrast, the tau level remaining in the pellet of mitotic cells was drastically reduced to about 22% due to detergent extraction (lanes 8 and 9). This result confirmed that tau becomes indeed detached from microtubules during mitosis. It is widely accepted that tau phosphorylation is a key factor regulating tau–microtubule interactions. Hence, we wanted to determine the phosphorylation sites responsible for the changes in tau–microtubule interaction during mitosis. We therefore performed a mitotic arrest in tau-transfected CHO cells since they allow separation of metaphase and remaining interphase

cells by mechanical shake-off, in contrast to LAN-5 cells where this procedure is not applicable.

In nonsynchronized CHO cell cultures, approximately 10–15% of the cells are mitotic. Synchronization with nocodazole arrests cells mainly in metaphase (DeBrabander *et al*., 1986; Jordan *et al*., 1992). Stably transfected CHO cells were treated with 0.4 μg/ml nocodazole while labeled with [^{32}P]-orthophosphate. Mitotic cells were separated from the remaining interphase cells by mechanical shake-off. Interphase and metaphase cells were analyzed separately with 2D thin-layer electrophoresis (TLE)/TLC (Figure 5). The sevenfold increase in phosphorylation in metaphase can be attributed to the occurrence of five additional phosphopeptides as well as a relative increase in the phosphorylation of T181, T212/T217, and S235 (compare Figure 5, a and b). Table 1 summarizes the relative intensities of the identified spots. Three of the additional five peptides could be identified as S202/T205*, S214, and T153 in similar comparative analyses as for nonsynchronized cells (Illenberger, unpublished results). The incorporation of an additional phosphate group into the peptide S202 (^{195}SGYSSPGSPGTPGSR^{209}), which is faintly seen in the interphase sample (Figure 5a), shifts this peptide to the more acidic position of S202/T205* (further left in the map). The asterisk indicates that this doubly phosphorylated peptide contains a phosphate at S202 plus another one at either T205, S199, or S198. Since the phosphorylation-dependent antibody AT-8 recognizes phosphorylated S202 and T205, this result confirms our earlier findings that AT-8 reactivity is only observed in mitotic cells (Preuss *et al*., 1995; hence our nomenclature of this peak as S202/T205*). The strong signal labeled S396/S404 in nonsynchronized cells (Figure 3), corresponding to the doubly phosphorylated peptide T386-R406, has disappeared from interphase and metaphase cells. Instead, two new spots have appeared closer to the anode (Figure 5b, short arrows), probably corresponding to this peptide in triply phosphorylated forms. These peptides would be recognized by the antibody PHF-1 (Otvos *et al*., 1994), which is known to immunostain mitotic cells (Pope *et al*., 1994; Preuss *et al*., 1995). The diffuse spot at the bottom of the interphase pattern labeled with an asterisk (*) has disappeared in metaphase (Figure 5, a and b). This spot contains peptides doubly phosphorylated at S46 and T50 (Figure 3b and Table 1). The pattern observed for tau protein from metaphase cells partly resembles the phosphorylation pattern of recombinant tau phosphorylated by the cyclin-dependent kinases cdc2 and cdk5 (see below, Figure 6, a and b). Since cdc2 activity is high in mitotic cells, it seems likely that this proline-directed kinase is involved in the in vivo phosphorylation of tau protein. It is notable that the fraction of phosphothreonine in mitotic cells, 33% of all sites, is much higher than in nonsynchronized cells (12%, unpublished results), indicating that the mitotic kinases preferentially phosphorylate TP motifs.

When comparing the signals in interphase and metaphase CHO cells (Figure 5, a and b) with the pattern from nonsynchronized CHO cells (Figure 3b), it becomes obvious that there are significant differences in signal intensities for certain spots (especially for S214 and T153, the latter being hardly visible in nonsynchronized cells; Figure 3b). In addition, not all signals found in the bulk analysis are represented by

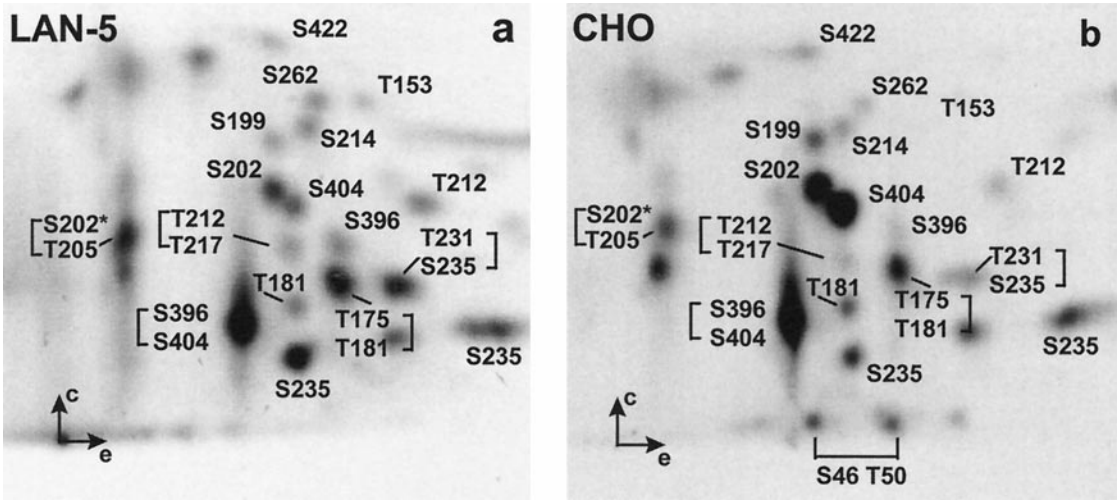

Figure 3. Analysis of tau phosphorylation in LAN-5 and CHO cell lines by 2D thin layer electrophoresis/chromatography. A portion of the tryptic digest (1000 cpm) was loaded per sample, and autoradiographs were exposed for 6 wk. (a) Tryptic phosphopeptide map of tau protein immunoprecipitated from transfected LAN-5 neuroblastoma cells. (b) Tryptic phosphopeptide map of endogenous tau protein immunoprecipitated from CHO cells.

Table 1. Identification of phosphorylated residues in vivo and in vitro

Spot		Sequence		LAN-5 relative intensity	CHO relative intensity	Interphase relative intensity	Metaphase relative intensity	cdc2	CDK5	MAPK	GSK3β	MARK
S46/T50[a]	25	KDQGGYT...	67	−	+	++	−			*	*	
S46/T50[b]	24	DQGGYT...	67	−	+	++	−			*	*	
T153	151	IATPR	155	+	(+)	−	+++	*	*	*		
T175	171	IPAKTPPAPK	180	−	−	−	−			*		
T181	175	TPPAPKTPPSSGEPPK	190	+	+	+	++			*		
T175/T181	171	IPAKTPPAPKTPPSSGEPPK	190	++	++	n.d.	n.d.			*		
S199[c]	195	SGYSSPGSPGTPGSR	209	+	++					*		
S202[d]	195	SGYSSPGSPGTPGSR	209	++	+++	+	−	*	*			
S202/T205*[e]	195	SGYSSPGSPGTPGSR	209	++	++	−	++	*	*	*		
T212	210	SRTPSLPTPPTR	221	+	+	n.d	n.d.	*	*	*		
T212/T217	210	SRTPSLPTPPTR	221	+	+	+	+++			*		
S214	212	TPSLPTPPTR	221	+	+	−	+++		*			
T231/S235	226	VAVVRTPPKSPSSAK	240	++	+	n.d.	n.d.	*				
S235[f]	231	TPPKSPSSAK	240	++	++	++	++	*	*	*		
S262	260	IGSTENLK	267	+	+	−	−					*
S293	291	CGSK	294	−	−	−	−					*
S324	322	CGSLGNIHHK	331	−	−	−	−					*
S356	354	IGSLDNITHVPGGGNK	369	−	−	−	−					*
S396	386	TDHGAEIVYKSPVVSGDTSPR	406	+	+	n.d.	n.d.			*		
S404	396	SPVVSGDTSPR	406	++	+++	++	+	*	*	*	*	
S396/S404[g]	386	TDHGAE...	−	++++	++++	−	−				*	
S422	407	HLSNVSSTGSIDMVDSPQ...	−	+	+	−	+			*		

*, Kinase phosphorylating this site; n.d., not determined; −, phosphorylation of this site not detected; + to ++++, phosphorylation detected with increasing intensity.

[a,b] Doubly phosphorylated peptides as determined by MALDI, equal amounts of P-Ser and P-Thr in phosphoamino acid analysis.

[c] S199 was determined for MAPK, but for the in vivo analysis it can only be concluded to be peptide 195-209 bearing a single phosphate.

[d] S202 was identified for cdc2 and cdk5; in the vivo analysis it corresponds to peptide 195-209 bearing a single phosphate.

[e] S202 with an additional phosphorylation at either S198, S199 or T205. Due to AT8 reactivity we conclude that this peptide is phosphorylated at S202 and T205.

[f] May occur at two different coordinates in the 2D maps.

[g] Doubly phosphorylated peptide as determined by MALDI, only P-Ser by phosphoamino acid analysis, containing a small fraction phosphorylated at S400.

simply adding interphase and metaphase signals. This is, for instance, the case for S262 (not visible in Figure 5), and for the pronounced spot S396/S404, which is only seen in nonsynchronized cells (not seen in Figure 5 but seen in Figure 3). This peptide could have partially acquired a further phosphate and therefore shifted to the left in Figure 5b (short arrows), or could, in part, be dephosphorylated (thus becoming invisible). These results suggest that the phosphorylation of tau protein is not only generally higher during mitosis, but furthermore, that tau is differentially phosphorylated during individual phases of mitosis, so that analyzing interphase and metaphase cells is not sufficient to generate all phosphopeptides that occur throughout the whole cell cycle. This would be consistent with the variations of microtubule dynamics during the phases of mitosis (e.g., Olmsted *et al*., 1989; Belmont *et al*., 1990), which could involve different states of tau phosphorylation.

Phosphorylation of tau In Vitro with Kinases cdc2, cdk5, MAPK, GSK-3β, and MARK, and Identification of Phosphorylation Sites

In principle, the phosphorylation sites in each spot of the in vivo maps could be identified by phosphopeptide sequencing using established procedures (Meyer *et al*., 1993). This would require at least 10 pmol of material (0.46 μg htau40, assuming phosphorylation is 100%), more than 1000 times the amount present in a spot of medium intensity. To circumvent this problem, we expressed tau in *E. coli*, phosphorylated it in vitro with several kinases in the presence of [γ-^{32}P]-ATP, and after tryptic digestion we separated the radiolabeled peptides by TLE/TLC and by HPLC chromatography, respectively. The HPLC experiments yielded sufficient material to identify the individual peptides by mass spectroscopy and sequencing. The spots in the 2D map were determined by running an aliquot of the total digest together with the identified

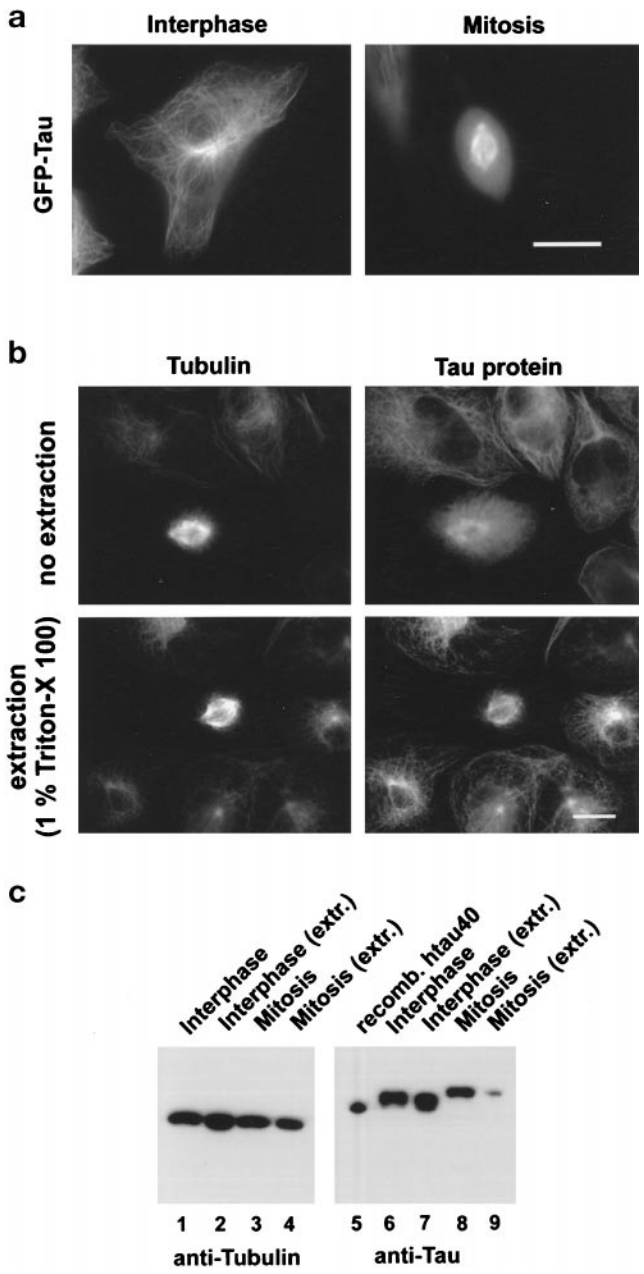

Figure 4. Tau–microtubule interaction in transfected CHO cells in interphase and during mitosis. (a) Observation of a living CHO cell expressing GFP-tau in interphase (left) and metaphase (right) CHO cell expressing GFP-tau. Bar, 20 μm. The increased cytosolic GFP-tau fluorescence in mitotic cells indicates that a large fraction of tau is not bound to microtubules during mitosis in contrast to interphase, where nearly all tau is associated with microtubules (exposure time of the metaphase cell was one-fifth of that for interphase cells, since when equal exposure times were used, mitotic cells would be overexposed and the mitotic spindle would not be discernible). (b) Indirect immunofluorescence analysis of CHO cells overexpressing the longest human tau isoform (htau40) without (upper panels) and after extraction (lower panels) with Triton X-100. No cytosolic stain, but only tau bound to the mitotic spindle, is observed after extraction (lower right). Tubulin staining with DM1A (left panels) and tau staining with polyclonal anti-tau antibody (right panels). Bar, 15 μm. (c) Western blot analysis of total cell extracts, lanes 1–4 DM1A against tubulin, lanes 5–9 T46 against tau protein. Tau levels in interphase cells are unaffected by extraction (lanes 6 and 7) whereas the tau signal is decreased to 22% in mitotic cells (lanes 8 and 9).

peptides (because of their higher concentration, the marker peptides could be identified in the mixture). Figure 6 shows experiments in which 400 μg of recombinant tau protein were phosphorylated with the kinases cdc2, cdk5, MAPK, GSK-3β (100 μg tau), and MARK. We chose cdc2 and cdk5 (Figure 6, a and b) because they have been shown to phosphorylate tau in vitro (Arioka *et al*., 1993; Baumann *et al*., 1993; Paudel *et al*., 1993), and because tau's phosphorylation is upregulated in mitotic CHO cells (Preuss *et al*., 1995). Since most of the phosphorylation sites detected by diagnostic phosphorylation-dependent PHF antibodies are of the SP or TP type, we also included mitogen-activated protein kinase (MAPK), which phosphorylates most of the SP or TP motifs in tau and is associated with microtubules (Drewes *et al*., 1992; Morishima-Kawashima and Kosik, 1996; Figure 6c), as well as GSK-3β (Figure 6d), which is known to be active in nonsynchronized cells (Woodgett, 1991; Mandelkow *et al*., 1992; Lovestone *et al*., 1994; Song and Yang, 1995). Finally, we chose MARK (Figure 6e) because it phosphorylates the KXGS motifs in the repeats, particularly S262, a residue that has a strong influence on tau's binding to microtubules (Biernat *et al*., 1993; Drewes *et al*., 1995; 1997) and shows elevated phosphorylation in AD (Morishima-Kawashima *et al*., 1995).

The kinases cdc2 and cdk5 show a rather similar phosphorylation pattern. Sites of major phosphate incorporation after phosphorylation with cdc2 (Figure 6a) comprise S202, S235, and S404 as well as the doubly phosphorylated peptides T231/S235 and S202/T205*. Minor signals were detected corresponding to peptides with phosphorylated T153 or T212. No phosphorylation at T231 could be observed for cdk5, since the peptide T231/S235 was missing (Figure 6b). Furthermore, T181, T175/T181, and S396 could be identified as additional phosphorylation sites. The non-proline-directed phosphorylation site S214 apparently generated by cdk5 is probably caused by a minor contamination with a different kinase since cdk5 was prepared from brain tissue. Phosphorylation with recombinant MAPK (activated by recombinant MEK) yielded 22 phosphopeptides. The following phosphorylation sites were identified: T153, T175, T181, T175/T181, S199, S202, S202/T205*, T212, T212/T217, S235, S396, S404, and S422. The prominent spots generated by GSK-3β (brief phosphorylation) include S404 and S396/S404 (containing a small fraction phosphorylated at S400), and in addition the doubly phosphor-

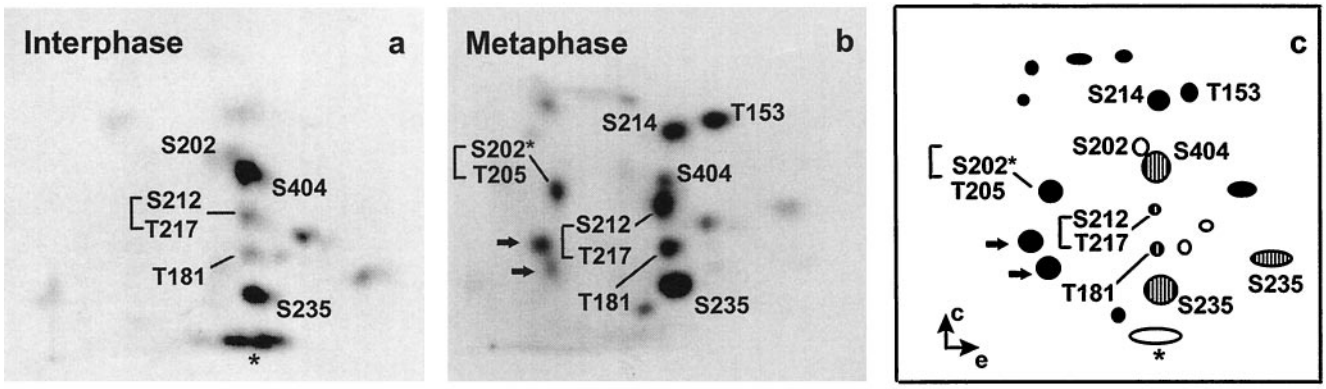

Figure 5. 2D maps of htau40 transfected CHO cells in interphase and metaphase. Cells were treated with 0.4 μg/ml nocodazole for 5 h. A portion (1000 cpm) of the tryptic digest was loaded per sample, and autoradiographs were exposed for 6 wk. (a) Interphase pattern revealing phosphorylation at T181, S202, S235, and S404. (b) Tau isolated from metaphase cells shows additional phosphorylation mainly at T153, S202/T205* (corresponding to the peptide 195–202 in htau40 bearing two phosphates), T212/217, S214, and two peptides (short arrows) corresponding to S386-R406 containing phosphorylated S396, S404, and another site. (c) Schematic diagram of phosphopeptides. Open circles represent signals present in interphase only, filled circles are phosphopeptides that only occur in metaphase, and gray circles are constitutively phosphorylated sites. The asterisks in Figure 5a represent the peptides containing phosphorylated S46 and T50 (see Figure 4b).

ylated peptides from the inserts (S46/T50), and S202/T205*. The spot S396/S404 is also the most prominent spot in nonsynchronized CHO and LAN-5 cells (Figure 3, a and b), consistent with the known activity of GSK-3β in interphase (Lovestone *et al*., 1994). The MAP/microtubule affinity-regulating kinase (MARK) mainly phosphorylates the KXGS motifs, S262, S293, S324, and S356, as published in Drewes *et al*., 1995. The identified phosphopeptides and corresponding kinases as well as relative intensities for signals identified in CHO and LAN-5 cells (compare Figures 3 and 5) are compiled in Table 1. These peptides served as a basis to interpret the phosphopeptide pattern of tau in cells and to identifiy 17 phosphorylation sites. Phosphopeptides in the in vivo samples were determined by running the samples shown in Figure 3 together with samples derived from in vitro phosphorylation with MAPK, MARK, and cdc2 (immunoprecipitated from mitotically arrested HeLa-S3 cells).

As an example for the analysis to identify in vivo phosphorylation sites, Figure 7 shows the comparison of the LAN-5 phosphorylation pattern with that of recombinant tau protein phosphorylated with a crude immunoprecipitate of cdc2 from mitotically arrested HeLa cells in vitro. Preliminary experiments (our unpublished data) had shown that if one immunoprecipitates cdc2 directly from supernatants of mitotically arrested HeLa cells, omitting the SP-Sepharose purification step, a S214- phosphorylating activity was also present in the immunoprecipitate. Therefore, we were able to use this "contaminated" fraction to investigate both the cdc2 pattern and the position of S214, irrespective of the kinase phosphorylating this residue. This explains why the pattern observed in Figure 7c differs from that in Figure 6a. However, this does not affect the identification of phosphopeptides since the identity of the peptides labeled in Figure 7c had been confirmed by additional in vitro analysis (our unpublished results). By comparing the in vivo pattern (Figure 7a) with the cdc2 pattern (Figure 7c) in the control run (Figure 7b, with aliquots of a and c run on the same plate), the following signals were identified: T153, T181, T175/T181, T212/T217, S214, T231/S235, S235, and S404. Similar analyses were conducted for both cell lines with MAP kinase, and MARK (our unpublished results). The prominent spot S396/S404 in both cell lines (Figure 3, a and b) was interpreted on the basis of the GSK-3β pattern (Figure 6d). Among the identified phosphopeptides, only four (T181, S202/T205*, T231/S235, and S396/S404) would be detected immunocytochemically with the monoclonal antibodies AT270, AT8, AT180, and PHF-1, respectively (Biernat *et al*., 1992; Goedert *et al*., 1995). Thus, the phosphopeptide maps confirm the increase of these antibody reactions during mitosis, and in addition they reveal the greater complexity of the phosphorylation of tau.

The Mitotic Phosphorylation Site Ser214 Strongly Affects the tau–Microtubule Interaction

In mitosis, microtubules are known to become highly dynamic (Belmont *et al*., 1990). At the same time, tau becomes hyperphosphorylated in transfected CHO cells (Preuss *et al*., 1995) concomitant with detachment of tau from microtubules (Figure 4). This led us to investigate whether the observed detachment of tau is due to its phosphorylation state. Among the phosphorylation sites elevated in nocodazole-treated cells, only S214 is not of the SP or TP type. In a previous

study (Trinczek *et al*., 1995) we had concluded that phosphorylation at SP or TP sites has only a moderate effect on the dynamic instability of microtubules in vitro, compared with others, such as S262 (in the KXGS motif of the first repeat; Biernat *et al*., 1993). We therefore wanted to determine directly the effect of the phosphorylation of S214 on the binding of tau to microtubules. S214 can selectively be phosphorylated by PKA in vitro, if appropriate conditions are chosen. By 15 min incubation time with PKA, almost 1 mol phosphate per mol tau is incorporated, and isolation and sequencing of the radioactive phosphopeptide show that phosphate incorporation occurs almost exclusively at S214 (Figure 8). Extended incubation times led to the incorporation of three to four phosphates by PKA, and these were distributed over more than 10 sites, including the KXGS motifs located in each of the repeats (S262, S324, S356).

The binding curves of Figure 9 show that the phosphorylation at S214 alone can account for the strong reduction in tau's affinity for microtubules (the dissociation constant K_d for phosphorylated tau protein is increased by approximately 10). Next, we asked whether this decrease in tau–microtubule interactions had any impact on microtubule stability. Figure 10 shows microtubule assembly monitored by video microscopy. The upper images show normal microtubule assembly in the absence of ATP (so that the added PKA remained inactive). However, when phosphorylation proceeds in the presence of ATP (Figure 10, bottom left), microtubule assembly is essentially suppressed. The effect is clearly due to the phosphorylation of S214 since the mutant Ser214Ala supports normal microtubule assembly, irrespective of phosphorylation by PKA (Figure 10, right). These data argue that the mitotic phosphorylation of S214 in tau could play a role in the detachment of tau from microtubules during mitosis and the concomitant increase in microtubule dynamics.

DISCUSSION

The interaction of tau and other MAPs with microtubules is regulated by phosphorylation, and this in turn affects the structure and dynamics of the microtubule cytoskeleton. In particular, tau becomes highly phosphorylated in the neurofibrillary pathology of Alzheimer's disease and hence loses its binding capability to

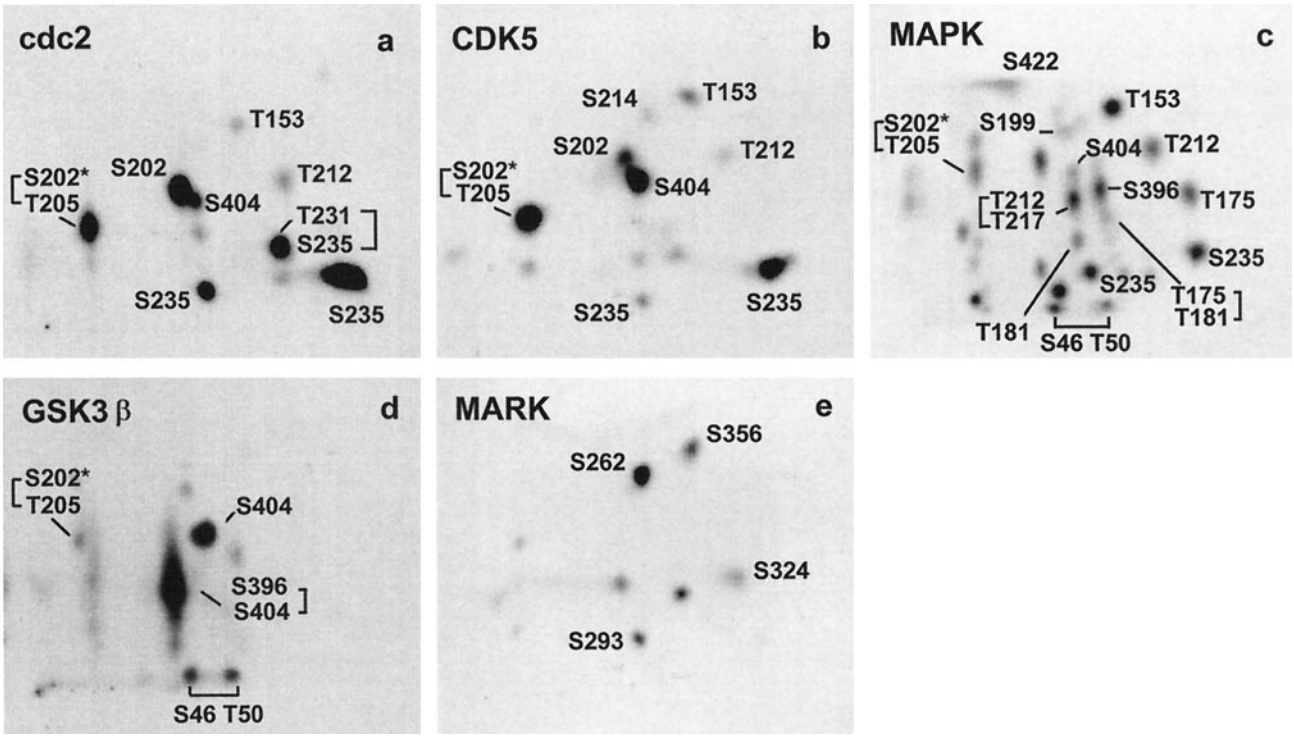

Figure 6. Tryptic 2D phosphopeptide maps of htau40 generated by different kinases in vitro. The peptides were obtained by tryptic digestion and separated by 2D TLE/TLC after phosphorylation. Aliquots of the tryptic digests (10.000 cpm per sample) were loaded and autoradiographs were exposed overnight. (a) htau40 phosphorylated with cdc2 immunoprecipitated from mitotically arrested HeLa-S3 cells for 16 h. (b) htau40 phosphorylated with cdk5, prepared from porcine brain (Baumann *et al*., 1993) for 16 h. (c) htau40 phosphorylated with recombinant MAPK (activated by MEK, Döring *et al*., 1993) for 16 h. (d) htau40 phosphorylated with recombinant GSK-3β for 1 h. (e) htau40 phosphorylated with MARK prepared from porcine brain (Drewes *et al*., 1995) for 2 h. Phosphorylation sites were identified by 2D analysis of HPLC-purified and sequenced peptides derived from the same phosphorylation assay for each kinase.

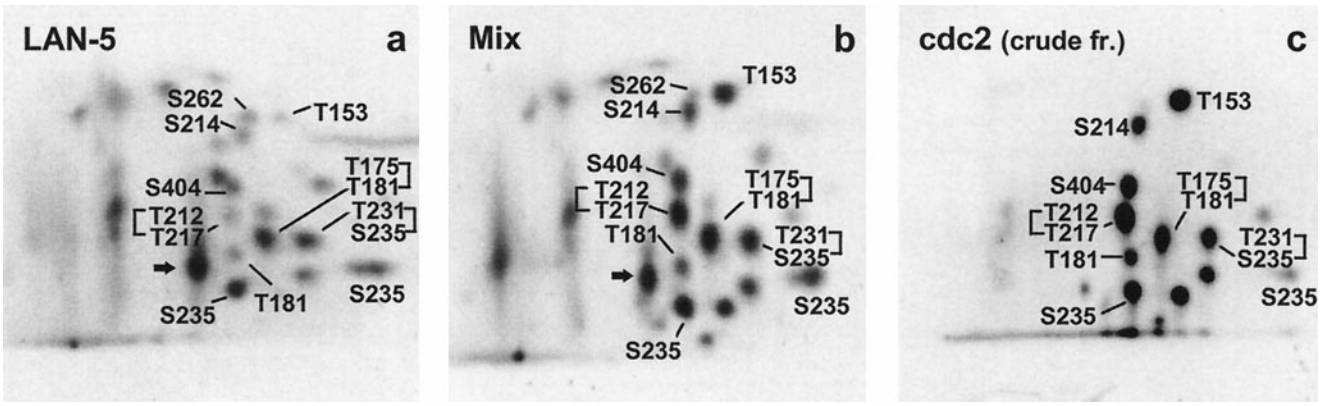

Figure 7. Identification of phosphopeptides generated in vivo, represented by the analysis of LAN-5 cells with tau phosphorylated with a crude fraction (see text for explanation) of cdc2. (a) 2D phosphopeptide map of tau from LAN-5 cells (same as in Figure 3a). (b) Control analysis with aliquots of the in vivo probe and of the cdc2 phosphorylated recombinant tau protein spotted onto the same plate. (c) In vitro sample of recombinant tau protein phosphorylated with cdc2 used in the control run in b. Phosphorylated residues are labeled; for identification of peptides see Table 1.

microtubules (Yoshida and Ihara, 1993). It has recently been discussed that the events leading to the abnormal phosphorylation of the MAP tau in AD involves mitotic mechanisms (Preuss *et al.*, 1995; Vincent *et al.*, 1996). Due to some insult yet to be identified, affected neurons may try to reenter the cell cycle. Since postmitotic neurons are unable to undergo cell division, this frustrated attempt finally leads to cell death and could explain the massive loss of neurons in AD. To investigate this hypothesis, we first had to check whether tau protein becomes detached from microtubules during mitosis in analogy with PHF-tau. Using three different methods, we could show that during mitosis a large fraction of tau becomes cytosolic (Figure 4) and that this is not due to a dramatic decrease in tubulin polymer (Figure 4c). This is in good agreement with studies showing that the level of tubulin polymer essentially remains constant throughout the cell cycle (Zhai and Borisy, 1994). In our previous investigation (Preuss *et al.*, 1995) we had already shown that the extent of tau phosphorylation is increased during mitosis and that tau presumably detaches from microtubules. However, to understand the role of phosphorylation, it is necessary to determine the specific phosphorylation sites of tau protein in living cells. In this study we therefore attempted to identify endogenous phosphorylation sites of the microtubule-associated protein tau in interphase and mitosis, as well as protein kinases that could be responsible for the phosphorylation. Many earlier studies aimed at phosphorylation sites in cells or tissues have relied on phosphorylation-dependent antibodies (reviews by Kosik and Greenberg, 1994; Trojanowski and Lee, 1995; Friedhoff and Mandelkow, 1998). However, these antibodies detect only a fraction of the potential phosphorylation sites, and in addition they are difficult to quantify, especially at low cellular concentrations. These limitations can be overcome by metabolic labeling of cells with ^{32}P and detection of phosphorylation sites by 2D phosphopeptide mapping.

Since many kinases are capable of phosphorylating tau in vitro (e.g., cdc2, cdk5, MAP kinase, GSK-3, PKA,

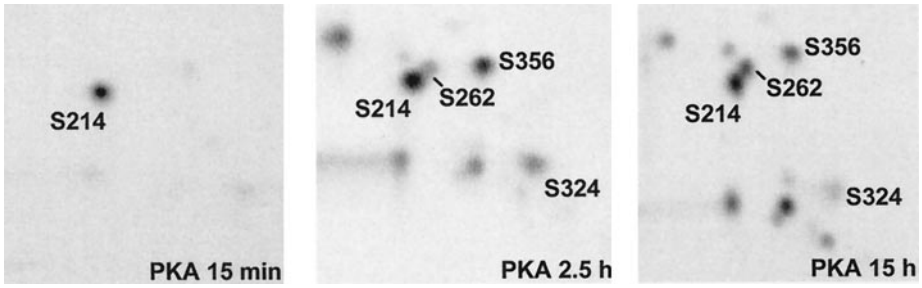

Figure 8. Phosphopeptide map of tau (htau23, 0.5 mg/ml) phosphorylated with PKA (1.5 U/μl) for (a) 15 min, (b) 2.5 h, (c) 15 h. Note that at 15 min nearly all phosphate is incorporated into Ser214. This condition was used for binding studies and the microtubule assembly assay (Figures 9 and 10).

MARK, for review see Mandelkow *et al*., 1995; Johnson and Jenkins, 1996), these experiments provide little information about the kinases phosphorylating tau in vivo. In our approach, however, they were valuable tools to generate reference phosphopeptides to identify phosphorylation sites in proliferating cells. In our experiments we included two members of the cell cycle-related kinase family, cdc2 and cdk5. Since cdc2 activity is up-regulated during mitosis, it seemed to be the most promising candidate for mitotic phosphorylation of tau protein in living cells as observed in our earlier study (Preuss *et al*., 1995). In postmitotic neurons, cdk5 is the most abundant kinase of the cdc2 family (Beaudette *et al*., 1993). Since the patterns of both kinases resemble one another, it is likely that cdks in general have a similar effect on tau in cells. Other potent kinases for tau are MAP kinase and GSK-3β, both of which are capable of phosphorylating many of the SP/TP sites and are associated with the microtubule network (Drewes *et al*., 1992; Hanger *et al*., 1992; Mandelkow *et al*., 1992; Morishima-Kawashima and Kosik, 1996; Roder *et al*., 1997). MARK is a novel kinase that has recently been described to phosphorylate tau protein in vitro and in vivo at S262 (Drewes *et al*., 1995, 1997), which has a pronounced effect on microtubule binding increasing microtubule dynamics (Biernat *et al*., 1993) and was therefore chosen as a non-proline-directed kinase.

LAN-5 neuroblastoma cells expressing moderate levels of the two smallest isoforms htau23 and htau24 (3 or 4 repeats, no inserts, Figure 2), and a CHO cell line transfected with htau40, the largest human isoform in the CNS, were investigated (Figures 1 and 2). Comparison of the overall phosphorylation pattern of tau in both cell lines revealed a surprising similarity in terms of tau phosphorylation irrespective of the different isoforms expressed (Figure 3) indicating similar kinase and phosphatase activities in both cell lines. This enabled us to use transfected CHO cells expressing tenfold more tau protein as a cell model to monitor tau phosphorylation in interphase and metaphase after nocodazole treatment (Figure 5). Moreover, with the phosphopeptides generated in vitro and sequenced we were able to identify 17 phosphorylation sites (Figures 6–8). Most of these (except S214 and S262) are of the SP/TP type, attesting to the activity of proline-directed kinases. Among the nonproline-directed motifs, S214 can be phosphorylated in vitro by PKA and to some extent by PKC (Steiner *et al*., 1990; Scott *et al*., 1993; Brandt *et al*., 1994) and S262 is phosphorylated mainly by MARK (Drewes *et al*., 1995, 1997) and to a lesser extent by PKA (Figures 6 and 8).

The bulk analysis of the phosphorylation sites (Figure 3) represents an average over the cell cycle, with about 10–15% of the cells undergoing mitosis at any time (this applies to both LAN-5 and CHO cells). Thus even sites that appear minor in the average population could play a major role at a particular stage or compartment. This question can be addressed only if one can subfractionate and compare different stages, such as interphase versus metaphase (see below). In support of this view, one should note that the overall extent of phosphorylation is quite low (2–3 phosphate groups per tau molecule, estimated from immunocytochemical analysis with phosphorylation-dependent antibodies (cf. Ksiezak-Reding *et al*., 1992; Köpke *et al*., 1993). This means that a given tau molecule is unlikely

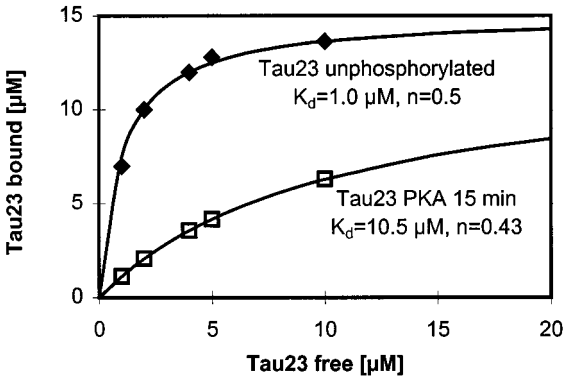

Figure 9. Binding of tau (isoform htau23) to microtubules (30 μM) before and after phosphorylation with PKA. Inserts, dissociation constant K_d and stoichiometry n. Conditions were chosen such that Ser214 is essentially the only phosphorylated residue (for details see Figure 8). Note that the phosphorylation strongly reduces the binding (K_d increases 10-fold).

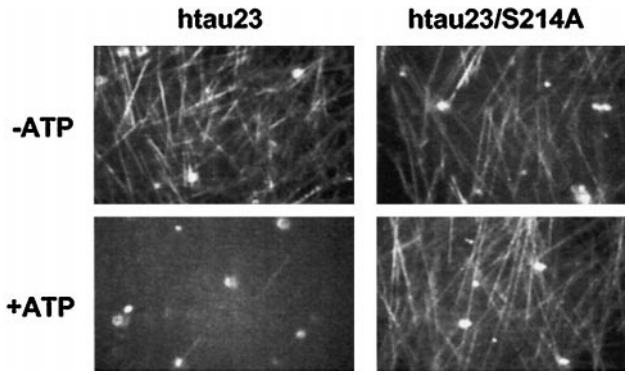

Figure 10. Dynamic instability of microtubules before and after phosphorylation of tau with PKA. The initial solution contained tubulin (25 μM), tau (10 μM), and PKA (1.5 U/μl, activity as in Figure 8). The images were taken 8 min after raising the temperature to 37°C. Left, isoform htau23; right, isoform htau23 with Ser214 mutated into Ala. Top, no ATP; bottom, prephosphorylated with 2 mM ATP. The top images show that microtubules grow well under the stabilizing influence of tau. The bottom left shows that microtubule formation is almost totally suppressed when PKA is allowed to phosphorylate tau (note that PKA has no direct effect on tubulin; our unpublished observations). The bottom right shows that the effect of PKA is mainly due to the phosphorylation of Ser214; when this residue is mutated to Ala, microtubules assemble normally.

to contain all of the phosphorylation sites detected in 2D phosphopeptide mapping. Direct evidence for this comes from the reactions with antibodies whose epitopes require a pair of phosphorylation sites, such as AT-8 (S202 and T205), AT-180 (T231 and S235), or PHF-1 (S396 and S404; Biernat *et al*., 1992; Otvos *et al*., 1994; Goedert *et al*., 1995). These antibodies are nearly undetectable in interphase (except PHF-1) but enhanced in mitosis (Pope *et al*., 1994; Preuss *et al*., 1995), implying that, at most, one but not both of their required sites is phosphorylated during interphase.

The mitotic arrest with nocodazole was performed in the transfected CHO cells, due to their significantly higher expression of tau protein. Phosphorylation of tau increases sevenfold during mitosis in transfected CHO and N2a cells (Preuss *et al*., 1995; Preuss and Mandelkow, 1998), particularly at T153, T181, S202/T205*, T212/T217, S235, and S214 (Figure 5). Except for S214 these sites are of the proline-directed type, particularly TP motifs. Considering the up-regulation of cdc2 during mitosis (for review see Stern and Nurse, 1996) and the fact that all the proline-directed sites are phosphorylated by this kinase in vitro, cdc2 is a strong candidate for causing the enhanced phosphorylation. However, strictly speaking, the up-regulation of other proline-directed kinases, or the down-regulation of tau phosphatases (particularly PP-2a and PP-2b, Drewes *et al*., 1993; Trojanowski and Lee, 1995; Wang *et al*., 1995; Merrick *et al*., 1996), cannot be excluded.

Mitosis is accompanied with a rearrangement of microtubules, higher dynamics, and a loosening of the MAP–microtubule interactions (Belmont *et al*., 1990; Verde *et al*., 1992; Ookata *et al*., 1995). If this is due to MAP phosphorylation, one would expect that some of the up-regulated sites have an influence on tau's binding to microtubules. Proline-directed phosphorylation does have an effect (Drechsel *et al*., 1992; Trinczek *et al*., 1995), but it is rather moderate, at least in vitro, when compared with the much larger effect of S262 phosphorylation (Illenberger *et al*., 1996; Drewes *et al*., 1997). It was therefore unexpected that the major increase at a non-proline-directed site in metaphase was at S214 and not at S262. Since PKA phosphorylates S214 in vitro (Scott *et al*., 1993; Brandt *et al*., 1994; Zheng-Fischhöfer *et al*., 1998), we further investigated whether this could have an effect on the interaction of tau with microtubules and on the dynamic behavior of microtubules in vitro. There was indeed a strong decrease in tau's microtubule binding and nucleation activity in vitro (Figures 9 and 10). This influence was eliminated when Ser214 was mutated into Ala. Thus, PKA or an equivalent kinase could contribute to the rearrangement of the microtubule network during mitosis. These results are consistent with recent results by Brandt *et al*. (1994) and Leger *et al*. (1997) showing the influence of PKA on tau's ability to bundle microtubules and support neurite outgrowth. PKA activity can be stimulated in situ in brain slices (Fleming and Johnson, 1995), and one of its effects is to increase the rate of axonal transport in neurons, possibly by phosphorylating tau and other MAPs (Sato-Harada *et al*., 1996). In addition to its direct effects, PKA could influence the tau–microtubule interaction indirectly by altering its susceptibility to other proline-directed kinases, e.g., MAP kinase or GSK-3 (Raghunandan and Ingram, 1995; Singh *et al*., 1995). The close association of PKA with the microtubule cytoskeleton is demonstrated by the observation that some MAPs (e.g., MAP2) provide anchoring sites for PKA (Obar *et al*., 1989; Faux and Scott, 1996). Interestingly, PKA can be detached and activated by phosphorylating their RII-regulatory subunit with cdc2 (Keryer *et al*., 1993). Furthermore, it has been shown that PKA activity is crucial for cell cycle progression, since blocking PKA activity in metaphase prevented the transition from mitosis to interphase (Grieco *et al*., 1996). We note, however, that S214 can also be phosphorylated by PKC, albeit with lower efficiency. Since some PKC isoforms are up-regulated in mitosis (Watanabe *et al*., 1992; Lehrich and Forest, 1994, Thompson and Fields, 1996), this kinase or a related one could also contribute to the increase in microtubule dynamics.

In the nonsynchronized cells, S262 is the only one of the four KXGS motifs phosphorylated. Our result is in good agreement with earlier observations by Seubert *et al*. (1995). In their immunocytochemical study with the phosphorylation-dependent antibody 12E8, which recognizes the phosphorylated KXGS motifs S262 and S356, respectively, they could show that only S262 was phosphorylated in fetal human brain tissue. S262 is the major target site for MARK in vitro (Biernat *et al*., 1993; Drewes *et al*., 1995) and in vivo (Drewes *et al*., 1997) and to a far lesser extent for PKA (Drewes *et al*., 1995). In addition, MARK also phosphorylates the closely related MAP2 and MAP4 at the corresponding, highly conserved KXGS motifs (Illenberger *et al*., 1996). All three MAPs fail to bind to microtubules upon phosphorylation by MARK, rendering microtubules highly dynamic. These data suggest that MARK is responsible for the phosphorylation at S262 in eukaryotic cells. Since phosphorylation at S262 is neither observed during interphase or metaphase in the cells (after mitotic arrest with nocodazole) and phosphorylation at this particular site is rather weak in the nonsynchronized cell population (Figure 2a), it is likely that this residue is only briefly phosphorylated during mitosis, possibly in prophase, where cellular microtubules are rearranged to form the mitotic spindle. By analogy, S214 has a similar low intensity in the bulk analysis, but gives a strong signal in metaphase (compare Figures 3 and 5). However, since the activation of MARK is not yet known, it remains to be shown that MARK is active in proliferating cells and that its activity is regulated during the cell cycle.

Finally, we note that the hyperphosphorylation and aggregation of tau protein (PHFs) is one of the hallmarks of AD pathology. Events that trigger the obvious imbalance of protein kinases and phosphatases in the affected neurons remain hitherto unknown. Several lines of evidence suggest that mitotic mechanisms might be involved, since earlier immunocytochemical studies have shown that tau protein from mitotic cells is recognized by phosphorylation-dependent antibodies diagnostic of Alzheimer neurofibrillary tangles (Pope *et al*., 1994; Preuss *et al*., 1995; Vincent *et al*., 1996). The present investigation supports these studies in that the phosphorylation pattern of tau in metaphase cells closely resembles that generated by cdc2 and cdk5 in vitro except for the non-proline-directed site S214. These results help explain why tau protein from fetal brain tissue shows a higher degree of phosphorylation (Kanemaru *et al*., 1992; Bramblett *et al*., 1993; Yoshida and Ihara, 1993) and can also be detected with the same PHF antibodies (Goedert *et al*., 1994; Matsuo *et al*., 1994; Seubert *et al*., 1995), because these cells also undergo mitosis during embryogenesis. Furthermore, the antibody MPM-2, a marker antibody for mitotic phospho-epitopes (Vandre *et al*., 1991), strongly reacts with neurofibrillary tangles (Vincent *et al*., 1996). These findings have led to the hypothesis that in AD the neurons may respond to some insult, such as ischemia, oxidative stress, or β-amyloid toxicity, by a final attempt to reinitiate mitosis. Since postmitotic neurons are incapable of reentering the cell cycle, activating mitotic protein kinases, with the cdks being the most prominent, may lead to cell death instead. This implies a tight relationship between the cell cycle and cell death machinery, which seem to converge at the level of cdks that show indeed increased activity in apoptosis (for reviews see King and Cidlowski, 1995; Pandey and Wang, 1995). Furthermore, it has been shown that increasing cdk activity in differentiated neuronal cell lines causes apoptosis (Meikrantz and Schlegel, 1996), whereas treating differentiated cells with mitotic inhibitors after nerve growth factor depletion prevents cell death (Farinelli and Greene, 1996; Park *et al*., 1996). Consistent with this, cdc2 is up-regulated in Alzheimer brain tissue (Vincent *et al*., 1997). In addition, our finding that S214 is highly phosphorylated in metaphase also strongly suggests mitotic mechanisms to be involved. S214 is a prominent site in PHF tau (Morishima-Kawashima *et al*., 1995) and is part of the epitope of the antibody AT100, which is the only specific antibody for Alzheimer tau so far known (Hoffmann *et al*., 1997; Zheng-Fischhöfer *et al*., 1998). Thus, the 2D phosphopeptide maps will provide a valuable tool with which to monitor changes in tau phosphorylation in neuronal cells exposed to various conditions (e.g., stress, kinase and phosphatase inhibitors) and help elucidate mechanisms leading to the hyperphosphorylation of tau protein in AD.

ACKNOWLEDGMENTS

We are grateful to U. Böning, B. Krüger, and K. Alm for excellent technical assistance and to H.E. Meyer and H. Korte (Ruhr-University, Bochum) for peptide sequencing during the initial stage of this work. The clone of GSK-3 was generously provided by J.R. Woodgett (Toronto, Ontario, Canada). The pEGFP-N1 vector was a generous gift from Dr. Pongs (ZMNH, Hamburg, Germany). The monoclonal antibody T46 was obtained from Dr. V.M.Y. Lee (University of Pennsylvania, Philadelphia, PA). This work was supported by a grant from the Deutsche Forschungsgemeinschaft.

REFERENCES

Arioka, M., Tsukamoto, M., Ishiguro, K., Kato, R., Sato, K., Imahori, K., and Uchida, T. (1993). Tau protein kinase II is involved in the regulation of the normal phosphorylation state of tau protein. J. Neurochem. *60*, 461–468.

Baumann, K., Mandelkow, E.-M., Biernat, J., Piwnica-Worms, H., and Mandelkow, E. (1993). Abnormal Alzheimer-like phosphorylation of tau by cyclin-dependent kinases cdk2 and cdk5. FEBS Lett. *336*, 417–424.

Beaudette, K., Lew, J., and Wang, J.H. (1993). Substrate specificity characterization of a cdc2-like protein kinase purified from bovine brain. J. Biol. Chem. *268*, 20825–20830.

Belmont, L.D., Hyman, A.A., Sawin, K.E., and Mitchison, T.J. (1990). Real-time visualization of cell-cycle dependent changes in microtubule dynamics in cytoplasmic extracts. Cell *62*, 579–589.

Biernat, J., Gustke, N., Drewes, G., Mandelkow, E.-M., and Mandelkow, E. (1993). Phosphorylation of serine 262 strongly reduces the binding of tau protein to microtubules: Distinction between PHF-like immunoreactivity and microtubule binding. Neuron *11*, 153–163.

Biernat, J., Mandelkow, E.-M., Schröter, C., Lichtenberg-Kraag, B., Steiner, B., Berling, B., Meyer, H.E., Mercken, M., Vandermeeren, A., Goedert, M., and Mandelkow, E. (1992). The switch of tau protein to an Alzheimer-like state includes the phosphorylation of two serine-proline motifs upstream of the microtubule binding region. EMBO J. *11*, 1593–1597.

Binder, L.I., Frankfurter, A., and Rebhun, L. (1985). The distribution of tau in the mammalian central nervous system. J. Cell Biol. *101*, 1371–1378.

Boyle, W.J., van der Geer, P., and Hunter, T. (1991). Phosphopeptide mapping and phosphoamino acid analysis by two-dimensional separation on thin layer cellulose plates. Methods Enzymol. *201*, 110–149.

Bramblett, G.T., Goedert, M., Jakes, R., Merrick, S.E., Trojanowski, J.Q., and Lee, V.M.Y. (1993). Abnormal tau phosphorylation at Ser(396) in Alzheimer's disease recapitulates development and contributes to reduced microtubule binding. Neuron *10*, 1089–1099.

Brandt, R., Lee, G., Teplow, D.B., Shalloway, D., and Abdelghany, M. (1994). Differential effect of phosphorylation and substrate modulation on tau's ability to promote microtubule growth and nucleation. J. Biol. Chem. *269*, 11776–11782.

Brion, J.P., Smith, C., Couck, A.M., Gallo, J.M., and Anderton, B.H. (1993). Developmental changes in tau phosphorylation: Fetal tau is transiently phosphorylated in a manner similar to paired helical filament tau characteristic of Alzheimers disease. J. Neurochem. *61*, 2071–2080.

Butner, K.A., and Kirschner, M.W. (1991). Tau-protein binds to microtubules through a flexible array of distributed weak sites. J. Cell Biol. *115*, 717–730.

Casnellie, J.E. (1991). Assay of protein kinases using peptides with basic residues for phosphocellulose binding. Methods Enzymol. *200*, 115–120.

DeBrabander, M., Geuens, G., Nuydens, R., Willebrords, R., Aerts, F., and DeMey, J. (1986). Microtubule dynamics during the cell cycle: the effects of taxol and nocodazole on the microtubule system of PtK2 cells at different stages of the mitotic cycle. Int. Rev. Cytol. *101*, 215–274.

Döring, F., Drewes, G., Berling, B., and Mandelkow, E.-M. (1993). Cloning and sequencing of a cDNA encoding rat brain mitogen activated protein (MAP) kinase activator. Gene *131*, 303–304.

Drechsel, D.N., Hyman, A.A., Cobb, M.H., and Kirschner, M.W. (1992). Modulation of the dynamic instability of tubulin assembly by the microtubule-associated protein tau. Mol. Biol. Cell *3*, 1141–1154.

Drewes, G., Lichtenberg-Kraag, B., Döring, F., Mandelkow, E.-M., Biernat, J., Goris, J., Doree, M., and Mandelkow, E. (1992). Mitogen-activated protein (MAP) kinase transforms tau protein into an Alzheimer-like state. EMBO J. *11*, 2131–2138.

Drewes, G., Mandelkow, E.-M., Baumann, K., Goris, J., Merlevede, W., and Mandelkow, E. (1993). Dephosphorylation of tau protein and Alzheimer paired helical filaments by calcineurin and phosphatase-2A. FEBS Lett. *336*, 425–432.

Drewes, G., Ebneth, A., Preuss, U., Mandelkow, E.-M., and Mandelkow, E. (1997). MARK—a novel family of protein kinases that phosphorylate microtubule-associated proteins and trigger microtubule disruption. Cell *89*, 297–308.

Drewes, G., Trinczek, B., Illenberger, S., Biernat, J., Schmitt-Ulms, G., Meyer, H.E., Mandelkow, E.-M., and Mandelkow, E. (1995). MAP/microtubule affinity regulating kinase (p110/mark): a novel protein kinase that regulates tau-microtubule interactions and dynamic instability by phosphorylation at the Alzheimer-specific site Serine 262. J. Biol. Chem. *270*, 7679–7688.

Farinelli, S.E., and Greene, L.A. (1996). Cell cycle blockers mimosine, ciclopirox, and deferoxamine prevent the death of PC12 cells and postmitotic sympathetic neurons after removal of trophic support. J. Neurosci. *16*, 1150–1162.

Faux, M.C., and Scott, J.D. (1996). Molecular glue-kinase anchoring and scaffold proteins. Cell *85*, 9–12.

Fleming, L.M., and Johnson, G.V.W. (1995). Modulation of the phosphorylation state of tau in situ: the roles of calcium and cyclic AMP. Biochem. J. *309*, 41–47.

Friedhoff, P., and Mandelkow, E. (1998). Tau Protein. In: Guidebook to the Cytoskeletal and Motor Proteins, ed. Th. Kreis and R. Vale, Oxford, England: Oxford University Press (*in press*).

Goedert, M., Jakes, R., Crowther, R.A., Cohen, P., Vanmechelen, E., Vandermeeren, M., and Cras, P. (1994). Epitope mapping of monoclonal antibodies to the paired helical filaments of Alzheimers disease: identification of phosphorylation sites in tau protein. Biochem. J. *301*, 871–877.

Goedert, M., Jakes, R., and Vanmechelen, E. (1995). Monoclonal antibody AT8 recognizes tau protein phosphorylated at both serine 202 and threonine 205. Neurosci. Lett. *189*, 167–170.

Goedert, M., Spillantini, M., Jakes, R., Rutherford, D., and Crowther, R.A. (1989). Multiple isoforms of human microtubule-associated protein-tau: Sequences and localization in neurofibrillary tangles of Alzheimers-disease. Neuron *3*, 519–526.

Goode, B.L., and Feinstein, S.C. (1994). Identification of a novel microtubule binding and assembly domain in the developmentally regulated inter-repeat region of tau. J. Cell Biol. *124*, 769–782.

Greenwood, J.A., and Johnson, G.V.W. (1995). Localization and in situ phosphorylation state of nuclear tau. Exp. Cell Res. *220*, 332–337.

Grieco, D., Porcellini, A., Avvedimento, E.V., and Gottesmann, M.E. (1996). Requirement for cAMP-PKA pathway activation by Mphase-promoting factor in the transition from mitosis to interphase. Science *271*, 1718–1723.

Gustke, N., Trinczek, B., Biernat, J., Mandelkow, E.-M., and Mandelkow, E. (1994). Domains of tau protein and interactions with microtubules. Biochemistry *33*, 9511–9522.

Hagestedt, T., Lichtenberg, B., Wille, H., Mandelkow, E.-M., and Mandelkow, E. (1989). Tau protein becomes long and stiff upon phosphorylation: Correlation between paracrystalline structure and degree of phosphorylation. J. Cell Biol. *109*, 1643–1651.

Hanger, D., Hughes, K., Woodgett, J., Brion, J., and Anderton, B. (1992). Glycogen-synthase kinase-3 induces Alzheimer's disease-like phosphorylation of tau: Generation of paired helical filament epitopes and neuronal localization of the kinase. Neurosci. Lett. *147*, 58–62.

Himmler, A., Drechsel, D., Kirschner, M., and Martin, D. (1989). Tau consists of a set of proteins with repeated C-terminal microtubule-binding domains and variable N-terminal domains. Mol. Cell. Biol. *9*, 1381–1388.

Hirs, C.H. (1967). Modification of cysteine residues. Methods Enzymol. *11*, 325–329.

Hoffmann, R., Lee, V.M.Y., Leight, S., Varga, I., and Otvos, L. (1997). Unique Alzheimer's disease paired helical filament specific epitopes involve double phosphorylation at specific sites. Biochemistry *36*, 8114–8124.

Hyman, A.A., and Karsenti, E. (1996). Morphogenetic properties of microtubules and mitotic spindle assembly. Cell *84*, 401–410.

Illenberger, S., Drewes, G., Trinczek B., Biernat, J., Meyer, H.E., Olmsted, J.B., Mandelkow, E.-M., and Mandelkow, E. (1996). Phosphorylation of microtubule associated proteins MAP2 and MAP4 by the protein kinase p110/mark: phosphorylation sites and regulation of microtubule dynamics. J. Biol. Chem. *271*, 10834–10843.

Johnson, G., and Jenkins, S. (1996). Tau protein and Alzheimer's disease brain. Alzheimer's Dis. Rev. *1*, 38–54.

Jordan, M., Thrower, D., and Wilson L. (1992). Effects of vinblastine, podophyllotoxin and nocodazole on mitotic spindles. Implications for the role of microtubule dynamics in mitosis. J. Cell Sci. *102*, 401–416.

Kanemaru, K., Takio, K., Miura, R., Titani, K., and Ihara, Y. (1992). Fetal-type phosphorylation of the tau in paired helical filaments. J. Neurochem. *58*, 1667–1675.

Kenessey, A., and Yen, S.H. C. (1993). The extent of phosphorylation of fetal tau is comparable to that of PHF tau from Alzheimer paired helical filaments. Brain Res. *629*, 40–46.

Keryer, G., Luo, Z.J., Cavadore, J.C., Erlichman, J., and Bornens, M. (1993). Phosphorylation of the regulatory subunit of type-ii-beta cAMP-dependent protein kinase by cyclin B/p34(cdc2) kinase impairs its binding to microtubule-associated protein-2. Proc. Natl. Acad. Sci. USA *90*, 5418–5422.

King, K.L., and Cidlowski, J.A. (1995). Cell cycle and apoptosis: common pathways to life and death. J. Cell Biochem. *58*, 175–180.

Köpke, E., Tung, Y., Shaikh, S., Alonso, A., Iqbal, K., and Grundke-Iqbal, I. (1993). Microtubule-associated protein tau: abnormal phosphorylation of a non-paired helical filament pool in Alzheimer's disease. J. Biol. Chem. *268*, 24374–24384.

Kosik, K.S., and Greenberg, S.M. (1994). Tau protein and Alzheimer disease. In: Alzheimer Disease, ed. R. Terry, R. Katzman, and K. Bick, New York: Raven Press, 335–344.

Kosik, K.S., and McConlogue, L. (1994). Microtubule-associated protein function: lessons from expression in *Spodoptera frugiperda* cells. Cell Motil. Cytoskel. *28*, 195–198.

Ksiezak-Reding, H., Liu, W.K., and Yen, S.H. (1992). Phosphate analysis and dephosphorylation of modified tau associated with paired helical filaments. Brain Res. *597*, 209–219.

Lee, G., Cowan, N., and Kirschner, M. (1988). The primary structure and heterogeneity of tau protein from mouse brain. Science *239*, 285–288.

Leger, J., Kempf, M., Lee, G., and Brandt, R. (1997). Conversion of serine to aspartate imitates phosphorylation-induced changes in the structure and function of microtubule-associated protein tau. J. Biol. Chem. *272*, 8441–8446.

Lehrich, R.W., and Forrest, J.N. (1994). Protein-kinase C-zeta is associated with the mitotic apparatus in primary cell cultures of the shark rectal gland. J. Biol. Chem. *269*, 32446–32450.

Li, W.P., Chan, W.Y., Lai, H.W.L., and Yew, D.T. (1997). Terminal dUTP nick end labeling (TUNEL) positive cells in the different regions of the brain in normal aging and Alzheimer patients. J. Mol. Neurosci. *8*, 75–82.

Lichtenberg-Kraag, B., Mandelkow, E.-M., Biernat, J., Steiner, B., Schröter, C., Gustke, N., Meyer, H.E., and Mandelkow, E. (1992). Phosphorylation dependent interaction of neurofilament antibodies with tau protein: epitopes, phosphorylation sites, and relationship with Alzheimer tau. Proc. Natl. Acad. Sci. USA *89*, 5384–5388.

Lovestone, S. *et al*. (1994). Alzheimers disease-like phosphorylation of the microtubule-associated protein tau by glycogen-synthase kinase-3 in transfected mammalian-cells. Curr. Biol. *4*, 1077–1086.

Ludin, B., Doll, T., Meili, R., Kaech, S., and Matus, A. (1996). Application of novel vectors for GFP-tagging of proteins to study microtubule-associated proteins. Gene *173*, 107–111.

Mandelkow, E.-M., Biernat, J., Drewes, G., Gustke, N., Trinczek, B., and Mandelkow, E. (1995). Tau domains, phosphorylation, and interactions with microtubules. Neurobiol. Aging *16*, 355–362.

Mandelkow, E.-M., Drewes, G., Biernat, J., Gustke, N., Van Lint, J., Vandenheede, J.R., and Mandelkow, E. (1992). Glycogen synthase kinase-3 and the Alzheimer-like state of microtubule-associated protein tau. FEBS Lett. *314*, 315–321.

Matsuo, E.S., Shin, R.W., Billingsley, M.L., Vandevoorde, A., Oconnor, M., Trojanowski, J.Q., and Lee, V.M.Y. (1994). Biopsy-derived adult human brain tau is phosphorylated at many of the same sites as Alzheimer's disease paired helical filament tau. Neuron *13*, 989–1002.

Meikrantz, W., and Schlegel, R. (1996). Suppression of apoptosis by dominant-negative mutants of cyclin-dependent protein-kinases. J. Biol. Chem. *271*, 10205–10209.

Melan, M.A., and Sluder, G. (1992). Redistribution and differential extraction of soluble proteins in permeabilized cultured cells. Implications for immunofluorescence microscopy. J. Cell. Sci. *101*, 731–743.

Merrick, S, E., Demoise, D.C., and Lee, V.M. (1996). Site-specific dephosphorylation of tau protein at Ser202/Thr205 in response to microtubule depolymerization in cultured human neurons involves protein phosphatase 2A. J. Biol. Chem. *271*, 5589–5594.

Meyer, H.E., Eisermann, B., Heber, M., Hoffmann-Posorske, E., Korte, H., Weigt, C., Wegner, A., Hutton, T., Donella-Deana, A., Perich, J.W. (1993). Strategies for nonradioactive methods in the localization of phosphorylated amino-acids in proteins. FASEB J. *7*, 776–782.

Morishima-Kawashima, M., Hasegawa, M., Takio, K., Suzuki, M., Yoshida, H., Titani, K., and Ihara, Y. (1995). Proline-directed and non-proline-directed phosphorylation of PHF-tau. J. Biol. Chem. *270*, 823–829.

Morishima-Kawashima, M., and Kosik, K.S. (1996). The pool of MAP kinase associated with microtubules is small but constitutively active. Mol. Biol. Cell *7*, 893–905.

Obar, R.A., Dingus, J., Bayley, H., and Vallee, R.B. (1989). The RII subunit of cAMP-dependent protein-kinase binds to a common amino-terminal domain in microtubule-associated proteins 2a, 2b, and 2c. Neuron *3*, 639–645.

Olmsted, J.B., Stemple, D., Saxton, W., Neighbors, B., and Mcintosh, J.R. (1989). Cell cycle-dependent changes in the dynamics of MAP2 and MAP4 in cultured-cells. J. Cell Biol. *109*, 211–223.

Ookata, K., Hisanaga, S., Bulinski, J.C., Murofushi, H., Aizawa, H., Itoh, T.J., Hotani, H., Okumura, E., Tachibana, K., and Kishimoto, T. (1995). Cyclin-B interaction with microtubule-associated protein-4 (MAP4) targets p34(cdc2) kinase to microtubules and is a potential regulator of M-phase microtubule dynamics. J. Cell Biol. *128*, 849–862.

Otvos, L., Feiner, L., Lang, E., Szendrei, G., Goedert, M., and Lee, V.M. (1994). Monoclonal antibody PHF-1 recognizes tau protein phosphorylated at serine residue 396 and 404. J. Neurosci. Res. *39*, 669–673.

Pandey, S., and Wang, E. (1995). Cells en route to apoptosis are characterized by the upregulation of c-fos, c-myc, c-jun, cdc2, and RB phosphorylation, resembling events of early cell-cycle traverse. J. Cell Biochem. *58*, 135–150.

Park, D., Farinelli, S.E., and Greene, L.A. (1996). Inhibitors of cyclin-dependent kinases promote survival of post-mitotic neuronally differentiated PC12 cells and sympathetic neurons. J. Biol. Chem. *271*, 8161–8169.

Paudel, H., Lew, J., Ali, Z., and Wang, J. (1993). Brain proline-directed protein kinase phosphorylates tau on sites that are abnormally phosphorylated in tau associated with Alzheimer's paired helical filaments. J. Biol. Chem. *268*, 23512–23518.

Pope, W.B., Lambert, M.P., Leypold, B., Seupaul, R., Sletten, L., Krafft, G., and Klein, W.L. (1994). Microtubule-associated protein-tau is hyperphosphorylated during mitosis in the human neuroblastoma cell-line SH-SY5Y. Exp. Neurol. *126*, 185–194.

Preuss, U., Döring, F., Illenberger, S., and Mandelkow, E.-M. (1995). Cell cycle dependent phosphorylation and microtubule binding of tau protein stably transfected into Chinese hamster ovary cells. Mol. Biol. Cell *6*, 1397–1410.

Preuss, U., and Mandelkow, E.-M. (1998). Mitotic phosphorylation of tau protein in neuronal cell lines resembles phosphorylation in Alzheimer's disease. Eur. J. Cell Biol. *in press*).

Raghunandan, R., and Ingram, V.M. (1995). Hyperphosphorylation of the cytoskeletal protein tau by the MAP-kinase PK40 (ERK2): regulation by prior phosphorylation with cAMP-dependent protein kinase A. Biochem. Biophys. Res. Commun. *215*, 1056–1066.

Roder, H.M., Fracasso, R.P., Hoffman, F.J., Witowsky, J.A., Davis, G., and Pellegrino, C.B. (1997). Phosphorylation-dependent monoclonal tau antibodies do not reliably report phosphorylation by extracellular signal-regulated kinase-2 at specific sites. J. Biol. Chem. *272*, 4509–4515.

Sato-Harada, R., Okabe, S., Umeyama, T., Kanai, Y., and Hirokawa, N. (1996). Microtubule-associated proteins regulate microtubule function as the track for intracellular membrane organelle transports. Cell Struct. Funct. *21*, 283–295.

Schliwa, M., Euteneuer, U., Bulinski, J.C., and Izant, J.G. (1981). Calcium lability of cytoplasmic microtubules and its modulation by

microtubule-associated proteins. Proc. Natl. Acad. Sci. USA *78*, 1037–1041.

Schoenfeld, T.A., and Obar, R.A. (1994). Diverse distribution and function of fibrous microtubule-associated proteins in the nervous system. Int. Rev. Cytol. *151*, 67–137.

Scott, C., Spreen, R., Herman, J., Chow, F., Davison, M., Young, J., Caputo, C. (1993). Phosphorylation of recombinant tau by cAMP-dependent protein kinase: identification of phosphorylation sites and effect on microtubule assembly. J. Biol. Chem. *268*, 1166–1173.

Seeger, R., Danon, Y., Rayner, S., and Hoover, F. (1982). Definition of a Thy-1 determinant on human neuroblastoma, glioma, sarcoma, and teratoma cells with a monoclonal antibody. J. Immunol. *128*, 983–989.

Seubert, P. *et al*. (1995). Detection of phosphorylated Ser(262) in fetal tau, adult tau, and paired helical filament tau. J. Biol. Chem. *270*, 18917–18922.

Singh, T.J., Haque, N., Grundke-Iqbal, I., and Iqbal, K. (1995). Rapid Alzheimer-like phosphorylation of tau by the synergistic actions of non-proline-dependent protein-kinases and GSK-3. FEBS Lett. *358*, 267–272.

Smale, G., Nichols, N.R., Brady, D.R., Finch, C.E., and Horton, W.E. (1995). Evidence for apoptotic cell death in Alzheimer's disease. Exp. Neurol. *133*, 225–230.

Song, J.S., and Yang, S.D. (1995). Tau-protein kinase-1 (GSK-3-beta, kinase Fa) in heparin phosphorylates tau on Ser(199), Thr(231), Ser(235), Ser(262) Ser(369), and Ser(400) sites phosphorylated in Alzheimer-disease brain. J. Protein Chem. *14*, 95–105.

Steiner, B. *et al*. (1990). Phosphorylation of microtubule-associated protein tau: identification of the site for Ca++-calmodulin dependent kinase and relationship with tau phosphorylation in Alzheimer tangles. EMBO J. *9*, 3539–3544.

Stern, B., and Nurse, P. (1996). A quantitative model for the cdc2 control of S phase and mitosis in fission yeast. Trends Genet. *12*, 345–350.

Studier, W.F., Rosenberg, A.H., Dunn, J.J., and Dubendorff, J.W. (1990). Use of T7 RNA polymerase to direct the expression of cloned genes. Methods Enzymol. *185*, 60–89.

Thompson, L.J., and Fields, A.P. (1996). Beta(ii) protein kinase-C is required for the G2/M phase transition of the cell-cycle. J. Biol. Chem. *271*, 15045–15053.

Trinczek, B., Biernat, J., Baumann, K., Mandelkow, E.-M., and Mandelkow, E. (1995). Domains of tau protein, differential phosphorylation, and dynamic instability of microtubules. Mol. Biol. Cell *6*, 1887–1902.

Trojanowski, J., and Lee, V.M.Y. (1995). Phosphorylation of paired helical filament-tau in Alzheimers disease neurofibrillary lesions: focusing on phosphatases. FASEB J. *9*, 1570–1576.

Vandre, D., Centonze, V., Peloquin, J., Tombes, R., and Borisy, G.G. (1991). Proteins of the mammalian mitotic spindle: phosphorylation-dephosphorylation of MAP-4 during mitosis. J. Cell Sci. *98*, 577–588.

Verde, F., Dogterom, M., Stelzer, E., Karsenti, E., Leibler, S. (1992). Control of microtubule dynamics and length by cyclin A-dependent and cyclin B-dependent kinases in *Xenopus* egg extracts. J. Cell Biol. *118*, 1097–1108.

Vincent, I., Jicha, G., Rosado, M., and Dickson, D.W. (1997). Aberrant expression of mitotic cdc2/cyclin b1 kinase in degenerating neurons of Alzheimers-disease brain. J. Neurosci. *17*, 3588–3598.

Vincent, I., Rosado, M., and Davies, P. (1996). Mitotic mechanisms in Alzheimers disease. J. Cell Biol. *132*, 413–425.

Wang, Q.M., Fiol, C.J., DePaoli-Roach, A.A., and Roach, P.J. (1994). Glycogen synthase kinase-3β is a dual specificity kinase differentially regulated by tyrosine and serine/threonine phosphorylation. J. Biol. Chem. *269*, 14566–14574.

Wang, J.Z., Gong, C.X., Zaidi, T., Grundke-Iqbal, I., and Iqbal, K. (1995). Dephosphorylation of Alzheimer paired helical filaments by protein phosphatase-2a and phosphatase-2b. J. Biol. Chem. *270*, 4854–4860.

Watanabe, T., Ono, Y., Taniyama, Y., Hazama, K., Igarashi, K., Ogita, K., Kikkawa, U., and Nishizuka, Y. (1992). Cell-division arrest induced by phorbol ester in CHO cells overexpressing protein kinase-C-delta subspecies. Proc. Natl. Acad. Sci. USA *89*, 10159–10163.

Woodgett, J.R. (1991). A common denominator linking glycogen metabolism, nuclear oncogenes, and development. Trends Biochem. Sci. *16*, 177–181.

Yoshida, H., and Ihara, Y. (1993). Tau in paired helical filaments is functionally distinct from fetal tau: Assembly incompetence of paired helical filament tau. J. Neurochem. *61*, 1183–1186.

Zhai, Y., and Borisy, G.G. (1994). Quantitative determination of the proportion of microtubule polymer present during the mitosis-interphase transition. J. Cell Sci. *107*, 881–890.

Zheng-Fischhöfer, Q., Biernat, J., Mandelkow, E.-M., Illenberger, S., Godemann, R., and Mandelkow, E. (1998). Sequential phosphorylation of tau protein by GSK-3β and protein kinase A at Thr212 and Ser214 generates the Alzheimer-specific epitope of antibody AT100 and requires a paired helical filament-like conformation. Eur. J. Biochem. *252*, 542–552.